Thao Nguyen

Capacitive Sensing: Water Level Application

Helsinki Metropolia University of Applied Sciences

Degree of Bachelor

Degree Programme in Electronics

Thesis

Date 24.05.2016

Helsinki Metropolia University of Applied Sciences

Author Title Number of Pages Date	Thao Nguyen Capacitive Sensing of Water Level 54 pages + 2 appendices 24 May 2016
Degree	Bachelor of Engineering
Degree Programme	Electronics
Specialisation option	Sensor
Instructors	Thierry Baills, Principal Lecturer Jan-Erik Eskelinen, Software Engineer

In this thesis, the application of capacitive sensing technology in liquid level monitoring will be analysed specifically. Applying the related techniques to design a sensor port of high sensitivity is the target which allows a high accuracy and reliability of measurement. The project involves improving the quality of the control signal by the capacitive sensor, which is demanded with several particular specifications in practice of a commercial product's design requirements. Therefore, the practicability of the project makes this paper being considered as a more applicable than theoretical document of technical research.

The implementation was taken advantage of approaches and methods. A wide source for a literature review was exploited for information collection of advanced capacitance calculation theory and existing applications of liquid level capacitive sensing. Expert and professional discussions were conducted on a regular basis of meetings with the instructors and the engineer team. Practical labs were substantially carried out for simulating and prototyping the sensor with computer-aid design programs and lab devices at school or company. Test codes were written in the online compiler - an integrated development environment on ARM mbed developer site.

The work results in digging deeper into the understanding of capacitive sensing, capacitance to digital conversion and their applications in water level tracking. Furthermore, it is satisfactory with a complete product of the sensor port, the sufficient accuracy of measurements and the first skills learned from designing a flexible printed circuit. Overall, the practice of the training process is fulfilled and preparatory for the valuable working experience and techniques of electronic systems designing and embedded systems programming in a coming future of a graduate in Electronics Engineering.

To sum up, this document can be used as an application note of advanced capacitive sensing technology for tracking the height level of any light viscosity fluid in a symmetrical-shaped reservoir. The specifications of capacitance to digital converter FDC1004 with inter-integrated circuit data transfer are also sharpened as a beneficial reference for a broad range of different applications using this capacitive sensing technology.

Keywords	liquid level, capacitive sensing, coplanar electrodes, CDC, I^2C

Contents

I. List of Figures

II. Index of Tables

III. List of Abbreviations

ACK	Acknowledgement
ADC	Analog to Digital Converter
ARM	Advanced RISC Machine
CAD	Computer-aid Design
CDC	Capacitance to Digital Converter
DUT	Devices under Test
FFC	Flat Flexible Cable
FPC	Flexible Printed Circuit
GUI	Graphic User Interface
I^2C	Inter Integrated Circuit
IC	Inter Integrated Circuit
IDE	Integrated Circuit
LSB	Least Significant Bit
mbed	Embedded System
MCU	Microcontroler
MSB	Most Significant Bit
OoP	Out of Phase
PC	Personal Computer
PCB	Printed Circuit Board
RE	Reference Environment
RL	Reference Liquid
RX	Receiver
SCL	Serial Clock
SDA	Serial Data
SDK	Software Development Kit
TX	Transmitter
USB	Universal Serial Bus

1 Introduction

This bachelor thesis includes overall documentation of my final year project work which was carried out for Finndent Company - a Finnish manufacturer of dental care units and patient chairs. Furthermore, the document is considered beneficial for development of professional studies at Helsinki Metropolia University of Applied Sciences.

The thesis project is to design and improve the accuracy of a capacitive sensor monitoring water level in the tank of a backflow prevention device which are needed to comply with European technical standards for dental care units. Capacitive sensing of liquid level is therefore a target to be studied in a deep revision of theoretical background. The reference of researches and developments of this technology mainly bases on Texas Instrument's technical documents accompanied with FD1004 capacitance to digital converter (CDC). As expected results, specifications of a flexible printed circuit (FPC) design of the sensor port and test codes written on an evaluation kit of Nucleo-F103RB microcontroller (MCU) are of primary discussion. However, the scope of this thesis is limited by the company secret as a part of the mother project and the other details of the existing prototype of the backflow prevention device are kept excluded in this document.

The backflow prevention device is designed to protect main supply water from contamination by the flow of used water back into clean water supply system due to, for example, pressure reduction in water supply line. In this prototype, main water is driven into water tanks in which the changes in the water level is sensed as input control signal used to command operations of air and water valve system to stabilize water flow rate at output. The more accuracy of sensors, the better control of pneumatic and water lines. Among several possible methods for sensing liquid level, capacitive sensing with symmetrical topology of coplanar conducting plates being contactless with the fluid is selected in design. Due to a high resolution of sensitivity for the expected quality of accuracy, capacitive effect of coplanar electrodes are in conditions meeting specific specification requirements of the product design. The water tanks came into the prototype in cylindrical shape and the clean water is kept as much touchless as possible by electrical and mechanical components. Therefore, the sensor port was designed as a FPC on which the coplanar sensor electrodes were embedded and easily bent into co-cylindrical shape surrounding the outside of the water tanks.

The specific scope of this thesis is to analyse the properties and specifications of:

- Coplanar capacitive sensor in a symmetrical topology, fringing effect and other design factors affecting its sensitivity,
- The FD1004 CDC configuration in out of phase (OoP) shielding mode for a high accuracy of measurements and
- Inter-integrated circuit (I^2C) communication of CDC signal between SMT32F103 microcontroller's peripheral and I^2C of FDC1004.

Obviously, the thesis project required a combination of the knowledge and techniques about sensors, computer-aid designs (CAD) and embedded systems (mbed). The theoretical analyses, the practical CAD design and test codes will be reported and discussed in details in the following sections.

2 Theoretical Background

Capacitive sensing is becoming a popular alternative to other methods in applications of proximity detection, material analysis and liquid level sensing. The main advantages that capacitive sensing has over other detection approaches are the capability to sense different kinds of materials (skin, plastic, metal, liquid etc.) together with specifications of being contactless and wear-free with a large sensing range, small design space of low cost PCB sensors and a low-power solution. To understand different types of applications and the constraints surrounding a system-level design entails, it is important to understand the theory of electrostatics and capacitance calculations. [1, 1.]

This theoretical revision covers: an analysis based on fringing effect of coplanar-plated capacitors; the way to adapt the capacitance sensing system into liquid level application with differential measurement of capacitance by a CDC; and the factors affecting the system to improve sensitivity of the sensor and accuracy of this measurement method. To be introduced first of all is an approach to a capacitor model consisting of two coplanar metallic foils whereof the capacitance can be considered approximately and similarly behaving in the co-cylindrical configuration with an appropriate bending angle.

2.1 Capacitance Approximation of Coplanar Electrodes

Under fringing effect, any changes in dielectric of surrounding environment can be detected by a capacitor consisting of a coplanar electrode pair. In this section, it is meant to investigate the effect and optimization of the geometric parameters of the electrodes to its high sensitivity. [2, 987.]

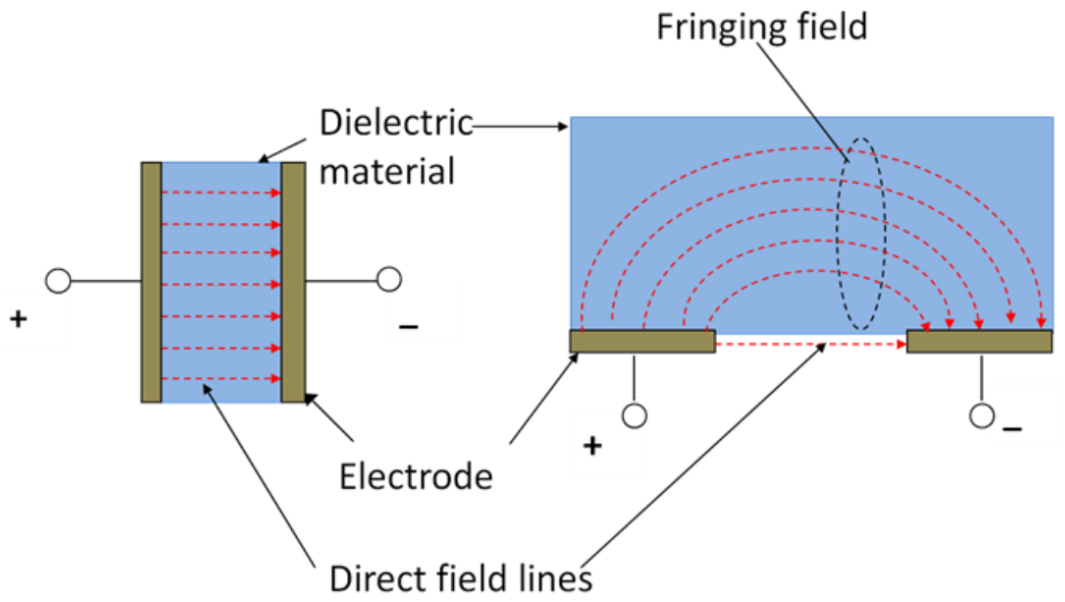

Figure 1. (a) Conventional parallel plate capacitor (b) Coplanar-plate capacitor [3, 10]

Capacitance (C) - a measurement of the capability to store an electrical charge (Q) in a body at a given voltage (V) is defined by:

$$C = \frac{Q}{V}$$

The capacitance of capacitive electrodes depends on the geometrical shape of the conductor-dielectric arrangement and position in the electric field [3, 9]. Figure 1 compares the differences of the capacitive electrodes in the coplanar structure with a conventional parallel plate capacitor whose capacitance is calculated by

$$C = \frac{\varepsilon_0 \varepsilon_r A}{d}$$

where ε_0, ε_r are vacuum permittivity and relative permittivity of the dielectric material in which the capacitor is immersed, A is area of the plate and d is the separation between the two parallel plates.

Coplanar electrodes can be mounted on most dielectric surfaces. “The fringing electric fields of the coplanar electrodes bend and penetrate into the material which is attached to the sensor. Thus, the variation of the dielectric property of the attached material affects the inter electrode capacitance.” [3, 9.] This will be proved soon.

The solution of the two dimension electric field of a model with a coplanar rectangular electrode pair of infinite length can be solved by *conformal mapping techniques* using the *inverse-cosine transform:*

$$W = V_0 - \frac{V_0}{\pi}\cos^{-1}\left(\frac{2Z}{a}\right) \tag{1}$$

by which a coordinate $Z = x + iy$ in the rectangular x-y plane is converted to $W = u(x,y) + iv(x,y)$ in the inverse cosine u-v plane, where the equipotential lines $u(x,y)$ are hyperbolic and the electrical flux lines $v(x,y)$ are elliptical. [4, 479.]

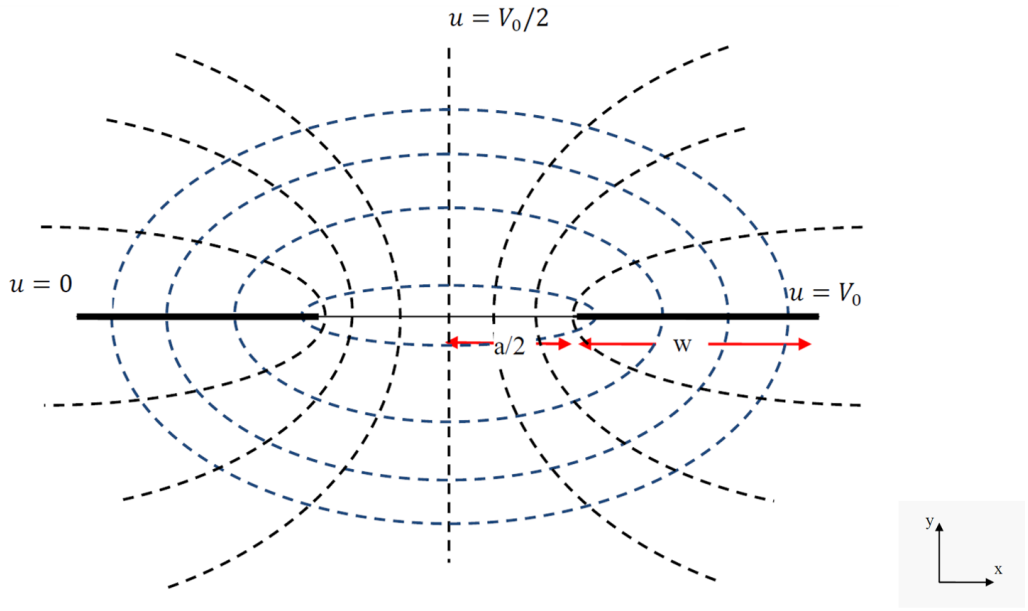

Figure 2. Two dimension Electric Fields between coplanar metal plates of an infinite length [3, 14]

Figure 2 depicts the two dimension electric field between coplanar electrodes where w - the electrode width, and a - the electrode gap separation can be seen in x-y plane; l - the electrode length (l >> w) not showed up is in z direction and V_0 represents the fixed potential difference between two electrodes.

Equation 1 can be rewritten as follows:

$$Z = \frac{a}{2}\cos\left(\frac{\pi}{V_0}(V_0 - W)\right)$$

$$x + iy = \frac{a}{2}\cos\left(\frac{\pi}{V_0}(V_0 - u) - i\frac{\pi}{V_0}v\right)$$

$$x + iy = \frac{a}{2}\cos\left(\frac{\pi}{V_0}(V_0 - u)\right)\cos\left(i\frac{\pi}{V_0}v\right) + \frac{a}{2}\sin\left(\frac{\pi}{V_0}(V_0 - u)\right)\sin\left(i\frac{\pi}{V_0}v\right)$$

$$x + iy = \frac{a}{2}\cos\left(\frac{\pi}{V_0}(V_0 - u)\right)\cosh\left(\frac{\pi v}{V_0}\right) + i\frac{a}{2}\sin\left(\frac{\pi}{V_0}(V_0 - u)\right)\sinh\left(\frac{\pi v}{V_0}\right)$$

Therefore, we have x, y coordinate values are translated in terms of u, v by [3, 15]:

$$x = \frac{a}{2}\cos\left(\frac{\pi}{V_0}(V_0 - u)\right)\cosh\left(\frac{\pi v}{V_0}\right) \tag{2}$$

$$y = \frac{a}{2}\sin\left(\frac{\pi}{V_0}(V_0 - u)\right)\sinh\left(\frac{\pi v}{V_0}\right) \tag{3}$$

Hence, the equations of elliptic and hyperbolic lines are derived as follows [3, 15]:

$$\frac{x^2}{\cosh^2\left(\frac{\pi v}{V_0}\right)} + \frac{y^2}{\sinh^2\left(\frac{\pi v}{V_0}\right)} = \frac{a^2}{4} \tag{4}$$

$$\frac{x^2}{\cos^2\left(\frac{\pi}{V_0}(V_0 - u)\right)} - \frac{y^2}{\sin^2\left(\frac{\pi}{V_0}(V_0 - u)\right)} = \frac{a^2}{4} \tag{5}$$

To solve the total electric charge on the electrodes, Gauss Law is applied [3, 20]:

$$Q = \iint D(y = 0)\cdot dA = 2l\int_{\frac{a}{2}}^{\frac{a}{2}+w} \left|D(y = 0)\right| dx \tag{6}$$

when all the electrical charges are assumed being located on the plane y = 0 (the electrode's surface) since the thickness of the electrode is negligible in comparison with its width. The electric displacement vector is defined by [3, 19]:

$$D = -\varepsilon_r\varepsilon_0\frac{\partial u}{\partial y}$$

$$D(y=0) = -\varepsilon_r \varepsilon_0 \left(\frac{\partial u}{\partial y}\right)_{y=0} \tag{7}$$

$\frac{\partial u}{\partial y}$ can be derived from differentiation of Equation 3 with respect to y:

$$\frac{2}{a} = -\frac{\pi}{V_0}\frac{\partial u}{\partial y}\cos\left(\frac{\pi}{V_0}(V_0 - u)\right)\sinh\left(\frac{\pi v}{V_0}\right) + \frac{\pi}{V_0}\frac{\partial v}{\partial y}\sin\left(\frac{\pi}{V_0}(V_0 - u)\right)\cosh\left(\frac{\pi v}{V_0}\right)$$

Then, the boundary condition of $u = V_0$ along the surface of the electrode $(a/2 \le x \le a/2 + w)$ on the plane y = 0 gives:

$$\left(\frac{\partial v}{\partial y}\right)_{y=0} = 0$$

$$\left(\frac{\partial u}{\partial y}\right)_{y=0} = -\frac{2V_0}{a\pi \sinh\left(\frac{\pi v}{V_0}\right)_{y=0}} \tag{8}$$

By substituting $\left(\frac{\partial u}{\partial y}\right)_{y=0}$ from Equation 8 into Equation 7 and Equation 6, we have:

$$D(y=0) = \varepsilon_r \varepsilon_0 \frac{2V_0}{a\pi \sinh\left(\frac{\pi v}{V_0}\right)_{y=0}}$$

$$Q = \frac{4\varepsilon_r \varepsilon_0 l V_0}{a\pi} \int_{\frac{a}{2}}^{\frac{a}{2}+w} \frac{dx}{\sinh\left(\frac{\pi v}{V_0}\right)_{y=0}} \tag{9}$$

The integrand in Equation 9 can be yielded as a function of x by solving Equation 2 at $u = V_0$ and y = 0:

$$x = \frac{a}{2}\cosh\left(\frac{\pi v}{V_0}\right)_{y=0}$$

Therefore,

$$\sinh\left(\frac{\pi v}{V_0}\right)_{y=0} = \sqrt{\left(\cosh\left(\frac{\pi v}{V_0}\right)_{y=0}\right)^2 - 1} = \sqrt{\left(\frac{2x}{a}\right)^2 - 1} \tag{10}$$

By substituting $\sinh\left(\frac{\pi v}{V_0}\right)_{y=0}$ from Equation 10 into Equation 9, we solve for Q:

$$Q = \frac{4\varepsilon_r\varepsilon_0 l V_0}{a\pi}\int_{\frac{a}{2}}^{\frac{a}{2}+w}\frac{dx}{\sqrt{\left(\frac{2x}{a}\right)^2 - 1}}$$

$$= \frac{2\varepsilon_r\varepsilon_0 l V_0}{\pi}\int_{\frac{a}{2}}^{\frac{a}{2}+w}\frac{\frac{2}{a}dx}{\sqrt{\left(\frac{2x}{a}\right)^2 - 1}}$$

$$= \frac{2\varepsilon_r\varepsilon_0 l V_0}{\pi}\int_{1}^{1+\frac{2w}{a}}\frac{dt}{\sqrt{t^2-1}};\left(t = \frac{2x}{a}\right)$$

$$= \frac{2\varepsilon_r\varepsilon_0 l V_0}{\pi}\ln\left[t + \sqrt{t^2-1}\right]_1^{1+\frac{2w}{a}}$$

$$Q = \frac{2\varepsilon_r\varepsilon_0 l V_0}{\pi}\ln\left[\left(1+\frac{2w}{a}\right) + \sqrt{\left(1+\frac{2w}{a}\right)^2 - 1}\right] \tag{11}$$

As a result, the capacitance of a coplanar electrode pair is:

$$C = \frac{Q}{V_0}$$

$$C = \frac{2\varepsilon_r\varepsilon_0 l}{\pi}\ln\left[\left(1+\frac{2w}{a}\right) + \sqrt{\left(1+\frac{2w}{a}\right)^2 - 1}\right] \tag{12}$$

$$C = \frac{2\varepsilon_r\varepsilon_0 l}{\pi}\ln\left[\frac{b}{a} + \sqrt{\left(\frac{b}{a}\right)^2 - 1}\right] \tag{13}$$

where $b = a + 2w$ is the electrode outermost edge separation [3, 21].

To evaluate the sensitivity of the coplanar electrode pair in different dimensions, the field penetration depth, T, is introduced as corresponding to the maximum y displacement of field line emanating from the outermost edge of the electrode pair [4, 474].

Solving Equation 3 at x = 0 and $u = \frac{V_0}{2}$ gives T as a function of v:

$$T = \frac{a}{2}\sinh\left(\frac{\pi v}{V_0}\right)_{y=T} \tag{14}$$

where v can be solved by applying to Equation 2 the boundary condition $x = \frac{a}{2} + w$ and $u = V_0$ when the maximum penetration occurs at the right most side of the electrode:

$$\frac{a}{2} + w = \frac{a}{2}\cosh\left(\frac{\pi v}{V_0}\right)_{y=T}$$

$$\sinh\left(\frac{\pi v}{V_0}\right)_{y=T} = \sqrt{\left(\cosh\left(\frac{\pi v}{V_0}\right)\right)_{y=T}^{2} - 1} = \sqrt{\left(1 + \frac{2w}{a}\right)^2 - 1} \tag{15}$$

Therefore,

$$T = \frac{a}{2}\sqrt{\left(1 + \frac{2w}{a}\right)^2 - 1} \tag{16}$$

$$T = \frac{a}{2}\sqrt{\left(\frac{b}{a}\right)^2 - 1} \tag{17}$$

Equations 16 and 17 indicate the field penetration depth is only dependent on the electrode geometric parameters [3, 16].

From Equations 13 and 17, the capacitance can be derived as a function of T:

$$C = \frac{2\varepsilon_r\varepsilon_0 l}{\pi}\ln\left[\frac{2}{a}\left(T + \sqrt{T^2 + 1}\right)\right] \tag{18}$$

Equation 18 is applied to the dielectric substrate of a thickness t >> T. It is implicated the capacitor is sensitive to dielectric change along z-axis. For example, each small change Δl of dielectric height from air to water causes the capacitance change an amount of:

$$\Delta C = \frac{2(\varepsilon_r - 1)\varepsilon_0 \Delta l}{\pi}\ln\left[\frac{2}{a}\left(T + \sqrt{T^2 + 1}\right)\right] \tag{19}$$

where $\varepsilon_r \approx 1$ for air and $\varepsilon_r \approx 80$ for water at 20^{0}C.

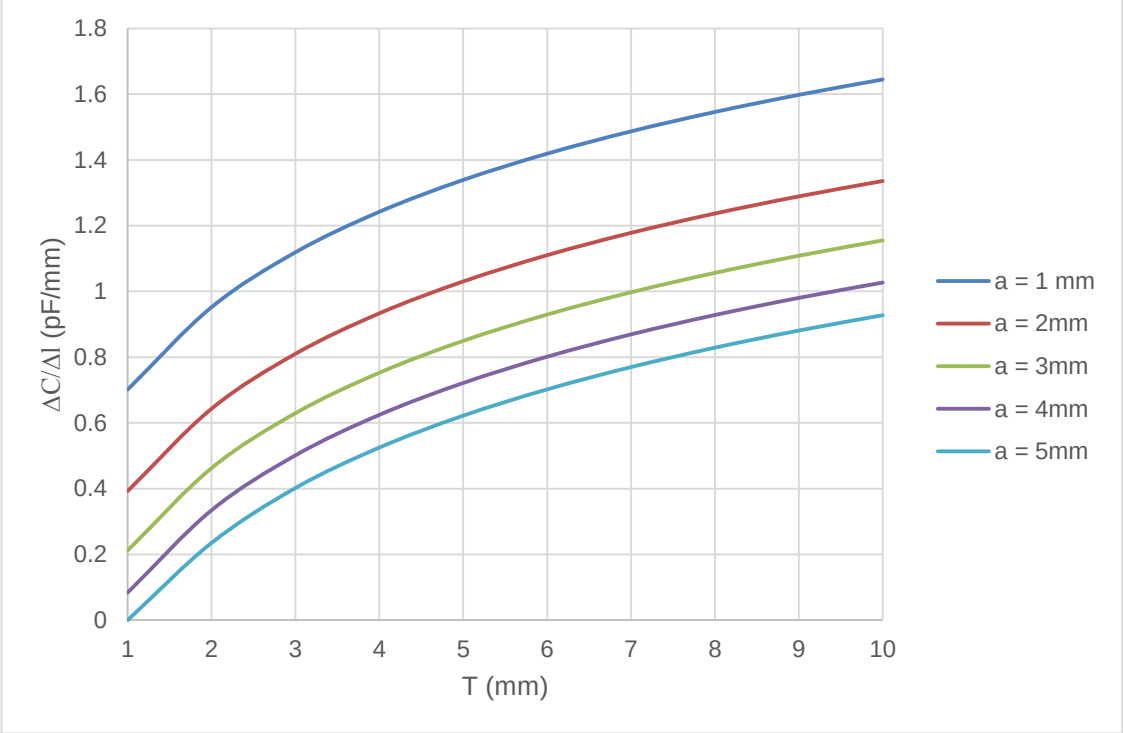

Figure 3. Capacitance change due to 1mm height change of dielectric from air to water of coplanar electrodes of infinite length.

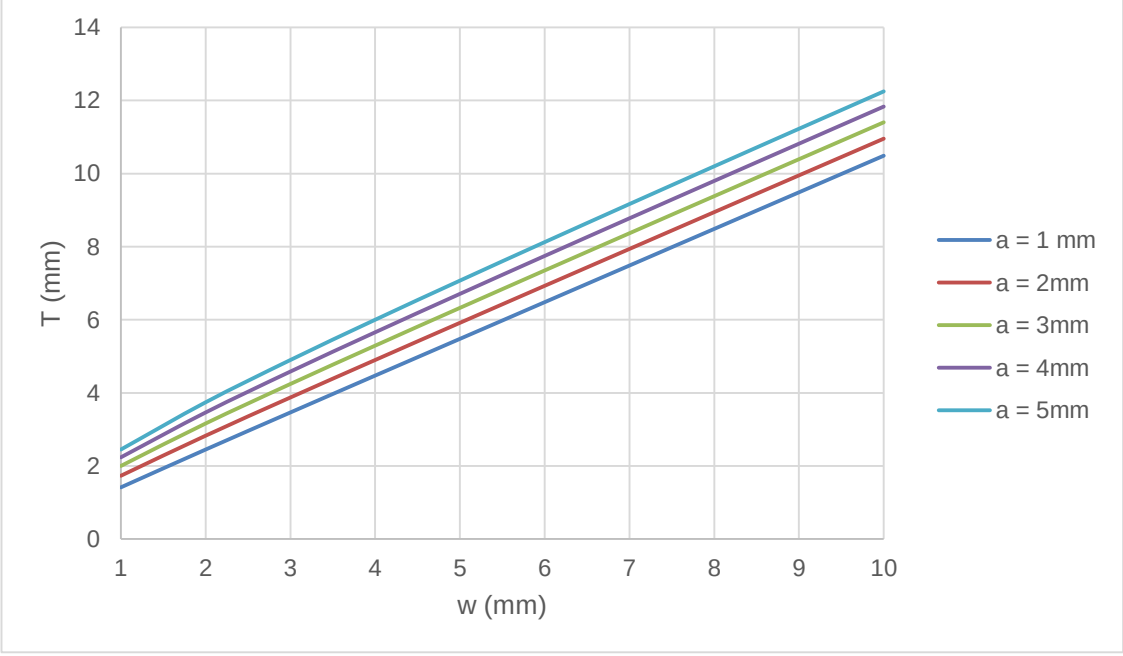

Figure 4. Field penetration depth versus electrode width of coplanar electrodes of different electrode gap.

Equation 19 indicates the more the dielectric height changes, the more the capacitance changes. Furthermore, the sensitivity of the electrodes depends on dielectric variation due to temperature drift. For example, dielectric permittivity of water has significant changes versus temperature. Figure 3 demonstrates rising sensitivity of coplanar electrodes with a shorter electrode gap and a longer field penetrate depth. Meanwhile, Equation 16 and Figure 4 illustrate that field penetrate depth is significantly maximized mainly by widening electrode width.

To sum up, optimization of the long coplanar electrodes for high sensitivity along z-axis involves minimizing the electrode gap separation and maximizing the field penetration depth by widening the electrode width. The condition is to be noticed that the thickness of dielectric material much more than the field penetration depth.

2.2 Liquid Level Capacitive Sensing

2.2.1 Liquid level coplanar-plate capacitive sensors

As analysed previously with fringing effect, the topology of a coplanar-plate capacitor allows itself adaptable for liquid level sensing application due to its high sensitivity to dielectric variation along z-axis. The electric field lines are dominant between the nearest edges of the electrodes and in the limit of the field penetration depth. Figure 5 illustrates the two dimension electric field line distribution of a model of 45mm-long, 6mm-wide and 2mm-separate copper coplanar-plate capacitor of 1-volt potential difference in air by COMSOL Multiphysics.

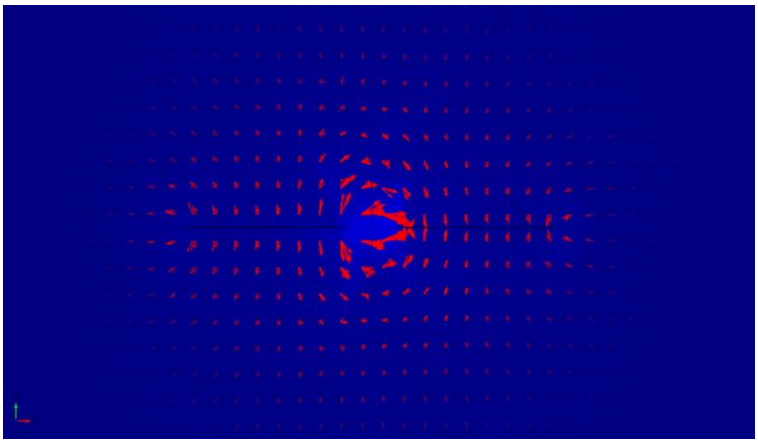

Figure 5. Two dimension plot of the electric field by a coplanar-plate capacitor modelled by COMSOL program

Here continues constructing a liquid level coplanar-plate capacitive sensor. The coplanar electrodes is now attached with a dielectric material on one of its sides with dielectric permittivity $\varepsilon = \varepsilon_r \varepsilon_0$ and geometric parameters of the electrodes and of the dielectric substrate are illustrated in Figure 6.

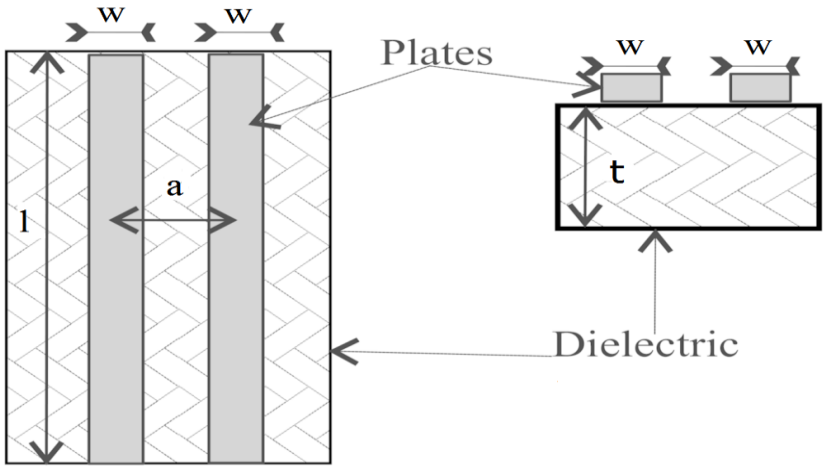

Figure 6. Coplanar electrodes attached with dielectric substrate on one of its side [5]

The capacitance due to the presence of the dielectric material on one of its side is given by [5]:

$$C = l \cdot \varepsilon \cdot \frac{K(k')}{2K(k)} \tag{20}$$

where $K(k)$ and $K(k')$ are *complete elliptic integrals of the first kind,*

k and k' are coefficients depending on the geometric parameters of the capacitor:

$$k' = \sqrt{1-k^2}$$

$$k = \frac{\tanh\left(\frac{\pi a}{4t}\right)}{\tanh\left(\frac{\pi(w+a/2)}{2t}\right)} = \frac{\tanh\left(\frac{\pi a}{4t}\right)}{\tanh\left(\frac{\pi b}{4t}\right)} \quad ;(b = 2w + a)$$

$$k \xrightarrow[t\to\infty]{} \frac{a}{b}$$

Equation 20 can be simply rewritten as [5]:

$$C = l \cdot \varepsilon \cdot f(a, w, t) \tag{21}$$

with $f(a,w,t)$ independent of the length of the plates or of the dielectric permittivity of the material.

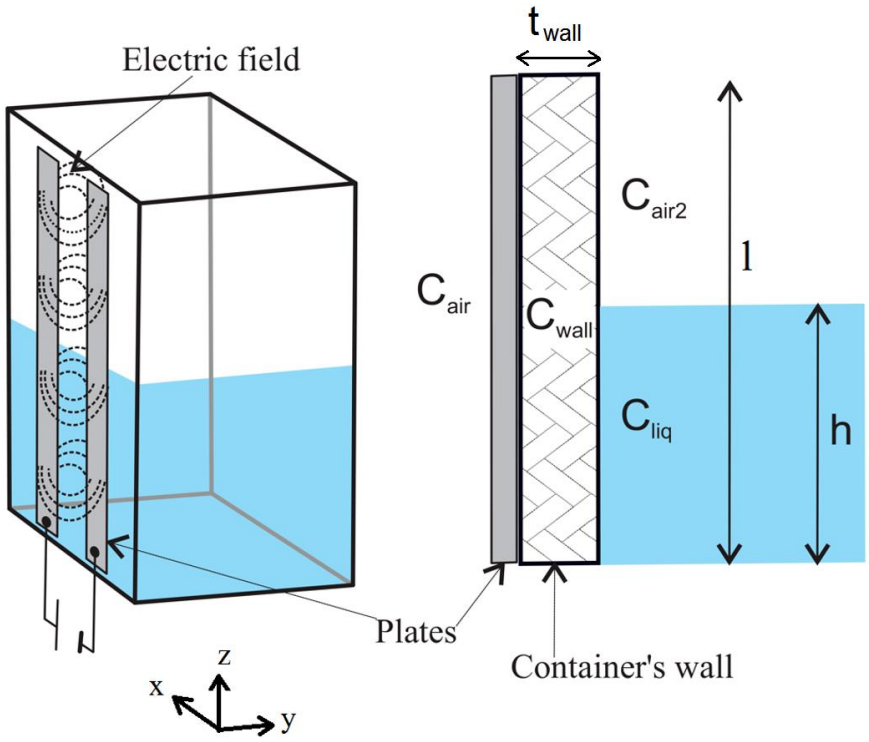

Figure 7. Multi-dielectric layers of liquid level sensing coplanar-plate capacitor [5]

Figure 7 illustrates the model of a liquid level sensing coplanar-plate capacitor which comprises multi dielectric layers. The total capacitance can be proved as a sum of four capacitance components:

$$C = C_{air} + C_{wall} + C_{liq} + C_{air2} \tag{22}$$

where C_{air} is the capacitance due to the presence of air outside the container, C_{wall} is the capacitance due to the container's wall, C_{liq} is the capacitance due to the height of the liquid column inside the container, and C_{air2} is the capacitance due to the presence of air in the upper part of the container. [5.]

Assumed with the infinite thickness of air and liquid, Equation 21 can be specifically expanded as:

$$C = l\varepsilon_{air} f(a,w,\infty) + l\varepsilon_{wall} f(a,w,t_{wall}) + h\varepsilon_{liq} f(a,w,\infty) + (l-h)\varepsilon_{air} f(a,w,\infty) \tag{23}$$

The capacitance of liquid level coplanar-plate capacitive sensor can be reduced as a function of the liquid height h:

$$C = C_0 + h\left(\varepsilon_{liq} - \varepsilon_{air}\right) f\left(a, w, \infty\right) = C(h) \tag{24}$$

where $C_0 = C(0)$ is the capacitance of the capacitive sensor when the container is empty. [5.]

2.2.2 Differential and Ratiometric Measurement of Liquid Level

Equation 24 implicates the capacitance of the liquid level coplanar-plate capacitive sensors depends on the dielectric variation due to environment changes (temperature shifts, humidity changes etc.) and makes a linear relationship with the liquid height. Therefore, setting up a measurement of the sensor capacitance independent of environment changes allows an accurate result of liquid level to be detected. Such a measurement can be implemented by a *ratiometric* and *differential measurement* setup as shown in figure below [1, 5].

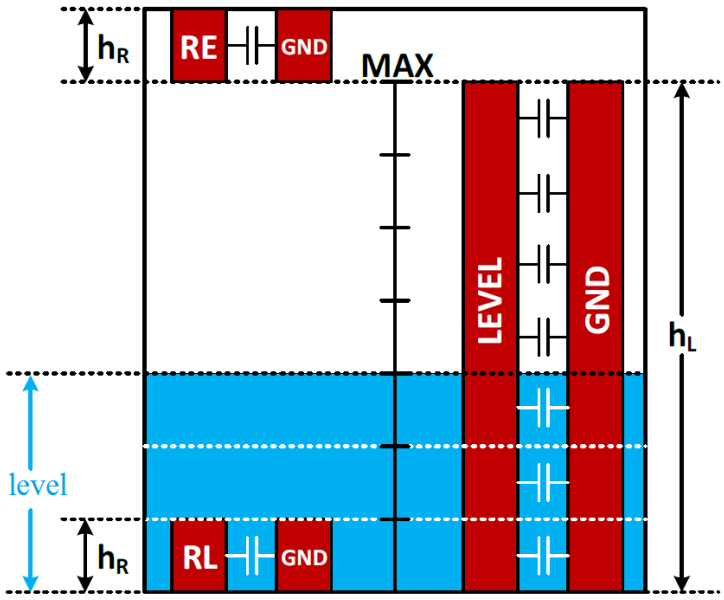

Figure 8. Differential and ratiometric measurement setup of liquid level sensing [6, 6]

In this setup, three coplanar-plate capacitive sensors are used (see Figure 8). The LEVEL electrode provides a capacitance value proportional to the height of the column of liquid (level). The Reference Environmental (RE) electrode and the Reference Liquid (RL) electrode are used as references. The RL electrode accounts for the liquid dielectric constant and its variation, while the RE electrode is used to compensate for any other environmental variations that are not due to the liquid itself. These sensors are

constructed with the electrodes being identical in width, thickness and gap separation but different in height (h_L for the LEVEL electrode height and the same h_R for the reference electrodes). [6, 6.]

The calculation of the electrode capacitances can be derived apparently from the Equations 23 and 24. The capacitance of the LEVEL electrode is given by:

$$C_{level} = C_{level0} + level\left(\varepsilon_{liq} - \varepsilon_{air}\right) f\left(a, w, \infty\right) = C_{level}(\varepsilon_{liq} - \varepsilon_{air}, h) \tag{25}$$

when the container is empty, h = 0 and

$$C_{level0} = C_{level}(\varepsilon_{liq} - \varepsilon_{air}, 0) \tag{26}$$

The general formula for the capacitance of the reference electrodes is:

$$C_{ref} = C_{ref\,0} + h\varepsilon_{liq} f(a, w, \infty) + (h_R - h)\varepsilon_{air} f(a, w, \infty) = C_{ref}\left(h\right) \tag{27}$$

When the container is full in the corresponding reference space of the RL electrode, the capacitance is:

$$C_{RL} = C_{ref}(h_R) = C_{ref\,0} + h_R \varepsilon_{liq} f\left(a, w, \infty\right) \tag{28}$$

The liquid level is always kept under the maximum level (MAX), which ensures an empty space in the container for tracking environmental changes of the RE electrode whose capacitance is:

$$C_{RE} = C_{ref}(0) = C_{ref\,0} + h_R \varepsilon_{air} f\left(a, w, \infty\right) \tag{29}$$

Combining Equations 28 and 29 gives:

$$C_{RL} - C_{RE} = h_R\left(\varepsilon_{liq} - \varepsilon_{air}\right) f\left(a, w, \infty\right) \tag{30}$$

As a result seen from Equations 25 and 30, the liquid level proportional to the unit height of the RL electrode is determined in a differential measurement by [6, 7]:

$$level = h_R \frac{C_{level} - C_{level0}}{C_{RL} - C_{RE}} \tag{30}$$

Where

- C_{RE} is the capacitance of the Reference Environmental electrode,
- C_{RL} is the capacitance of the Reference Liquid electrode,
- C_{level} is the current value of the capacitance measured at the Level electrode sensor,
- C_{level0} is the capacitance of the Level electrode when the container is empty, and
- h_R is the mutual height of Reference electrodes as the desired unit.

In a differential measurement, the presence of RE sensor is needed to track variation in dielectric due to changes in temperature, humidity and pressure on the material [1.5]. However, for relative accuracy of measurements with no concerns of environmental changes, the RE electrode can be taken out of the system and the liquid level is calculated as follows:

$$\text{level} = h_R \frac{C_{level} - C_{level0}}{C_{RL} - C_{RL0}} \tag{31}$$

where C_{RL0} is the capacitance of the RL electrode when the container is empty. Liquid level measurement with absence of RE sensor justifies its ratiometric specification since the level is mainly approximate to the capacitance proportion between the LEVEL and RL sensors in the height unit of the RL sensor.

The capacitance of the electrodes can be measured by a CDC. Here used the FDC1004 chip with the ability of configuration up to 4 capacitance measurements specialized for this application of liquid level in differential mode. The FDC1004 features and theory of operation will be described in more details of the following sections. The differential measurement of liquid level with the FDC1004 can be set up using active shielding and OoP liquid level technique.

2.2.3 Active Shielding

It is also implicated from Equations 19 and 21 that the fringing capacitance of a coplanar-plate capacitor is changing depends on variation in height (z-axis) and thickness (y-axis) of the dielectric material to which the capacitor is attached. If both electrodes of the sensor are shielded properly, it is intended to eliminate the electric field of the sensor electrodes on the shielded side and then focus sensing direction toward the liquid target. Additionally, the shield provides a barrier from any interference affecting the measurements of the sensor capacitance from the backside. [6, 7.]

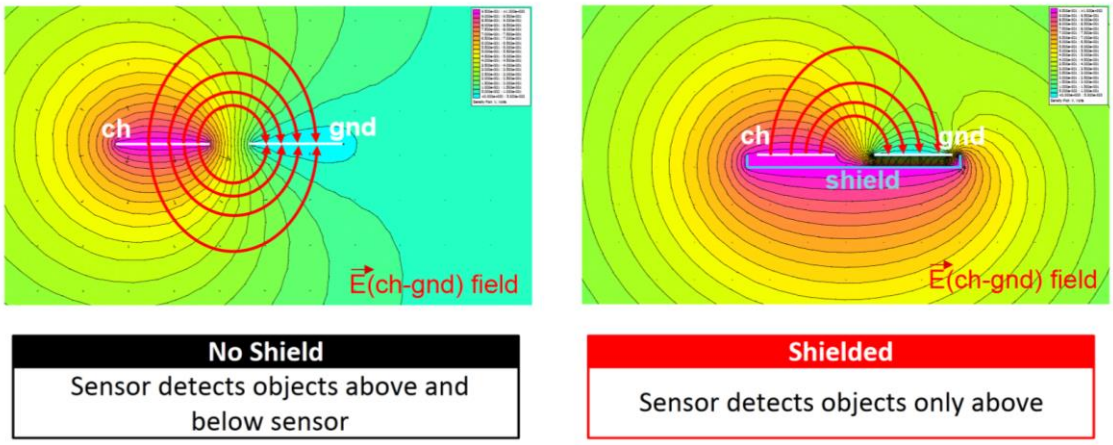

Figure 9. Shielding effect on the electric field of the sensor (ch) and ground (gnd) electrodes [7, 2]

The simplified model without care of fringing effects on the electrode edges in Figure 9 illustrates the effect of a shield behind both sensor electrodes. The shield is driven at the same voltage potential of the sensor electrode. Any external interference from the backside coupling to the shield has minimal interaction with the sensor electrode. Moreover, the electric field between the electrodes (red lines) are blocked on the shielded side, which reduces and directs the sensing angle to the target. Without the shield, the sensing angle of the sensor picks up any stray interference within the field-line vicinity. Depending on the shape and position of the shield relative to the sensor, the sensing angle can be more focused with a larger and closer shield to the sensor electrode (see Figure 10). [7, 2.]

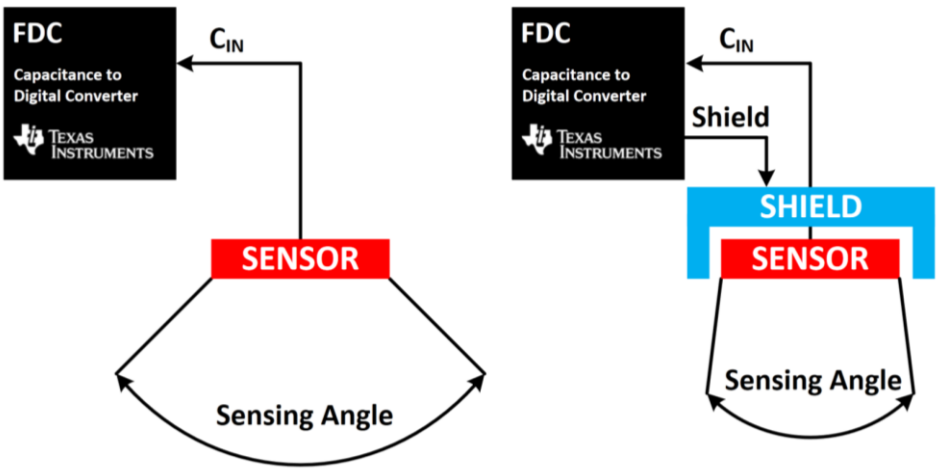

Figure 10. Focusing the sensing area of the sensor electrode with a shield [7, 3]

When connected to a CDC to measure the sensor capacitance, the parasitic capacitance due to the external circuity and connection between the sensor electrodes and the CDC pins is included in the measurement results. The parasitic capacitance in some cases can be larger than the sensor capacitance itself and significantly affected by environmental interferences, which results in drifts likely compromising the system accuracy. For instance, a long sensor-FDC1004 connection path produces a large parasitic capacitance, which slows down discharging time of the capacitor and may leads to the phenomenon of residue capacitance included in the measurement results. To eliminate the parasitic capacitance, active shielding is again a good solution. [8, 10.]

2.2.4 Out-of-Phase Liquid Level Technique

Despite of applying active shielding, the differential measurement of the sensor capacitances to ground of the conventional liquid level technique has still a considerable problem with the introduction of human body effect. Figure 11 describes a conventional electric model of liquid level measurement by FDC1004 and the human body effects as a ground interference source in the sensing area of the sensors [9, 5].

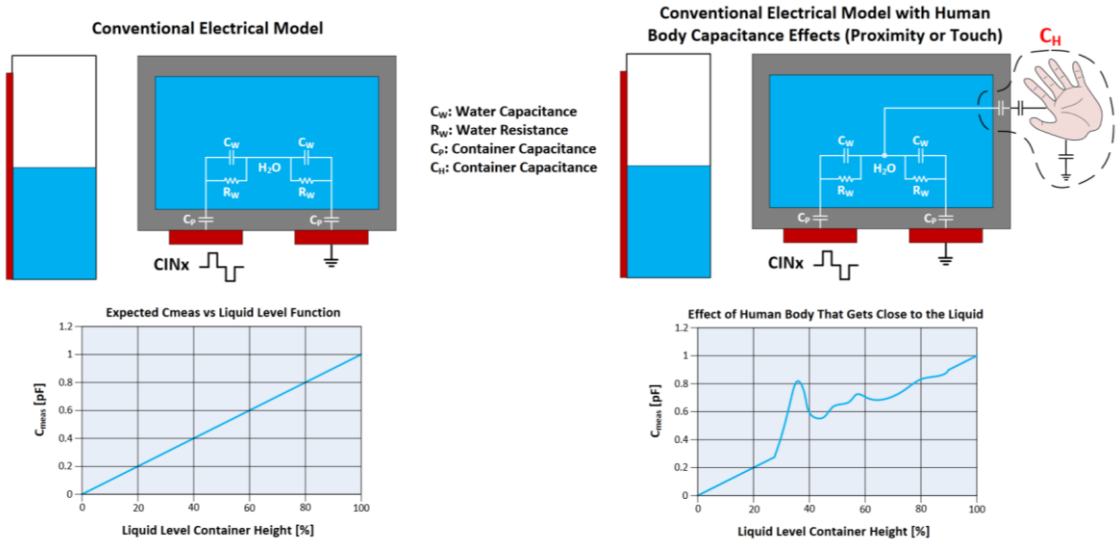

Figure 11. Conventional liquid level technique by FDC1004 suffering human body effect [9, 5]

As mentioned previously, the symmetry in the topology of the coplanar electrodes keep an important role in the liquid level sensing application. When applied with a driving shield, the sensing area is focused to the liquid target and immune to external

interferences on the shielded side. However, the presence of human body in the sensing area destroys the symmetry of the conventional electrical model and seriously affects the measurement accuracy.

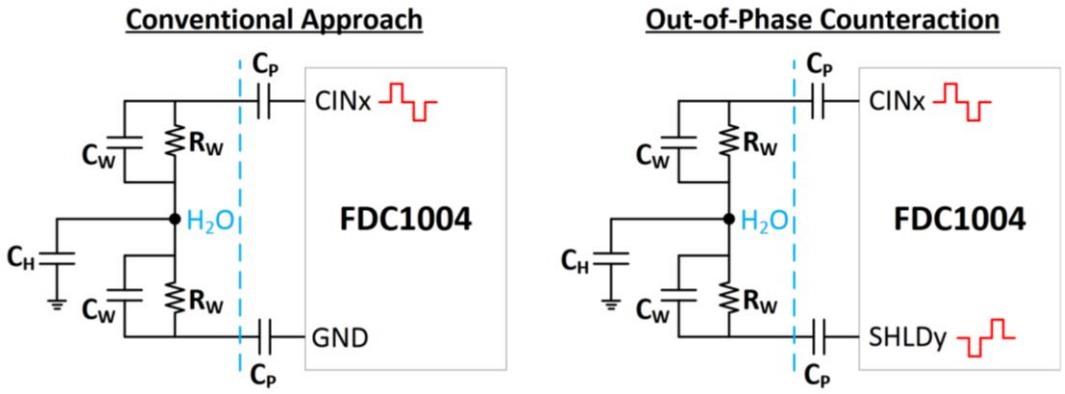

Figure 12. Comparison of conventional and OoP electrical model in liquid level application [9, 6]

The cause of this problem arises from the sensor electrode being excited by a signal waveform in most CDCs, that means the liquid experiences a varying voltage potential difference to ground during excitation phases. When the human body occurs as a ground interference source, an extra parasitic capacitance owing to human body (C_H) couples to the liquid. The value of this parasitic capacitance changes due to the liquid potential variation. These changes impose deviations in capacitance measurements and contribute the asymmetry of the conventional electric model. To neutralize the human body effect, the OoP technique is introduced to replace the conventional approach in the liquid level application. Figure 12 justifies the liquid potential is kept constant over time with replacement of the ground (GND) electrode by the OoP sensor (SHLDy) electrode which is excited in 180^0 out of phase with the sensor (CINx) electrode. The liquid potential remained constant by in-phase and out-of-phase excitation signals on the electrodes is to fix the human capacitance and preserve the symmetry of the electrical model. [9, 6.]

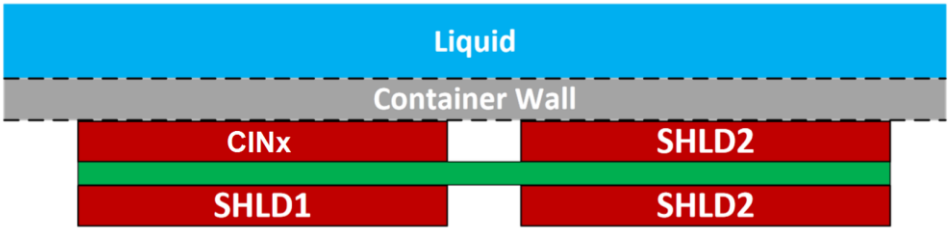

Figure 13. OoP technique sensor layout for LEVEL and REF sections [9, 7]

In OoP liquid level technique, the differential measurement setup with the FDC1004 uses two active shield electrodes as shown in Figure 13. The sensor electrode and its shield are driven in-phase with CINx and SHLD1 signal. The OoP sensor electrode and its shield are excited by the same SHLD2 signal. [9, 7.]

2.3 FDC1004 Capacitance to Digital Conversion

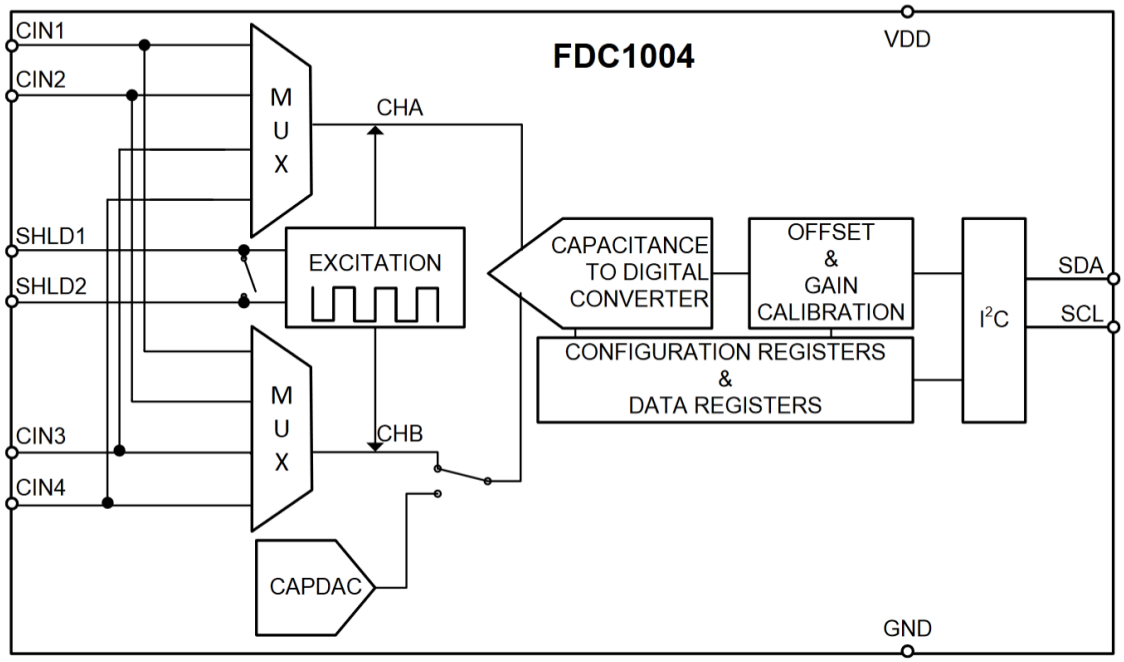

Figure 14. FDC1004 block diagram [8, 10]

The FDC1004 is a dedicated CDC with 4 input chanels (CIN1-4) which can be configured to measure up to 4 single capacitances in different applications (see Figure 14). Each input chanel can be selected to chanel CHA or CHB by a multiplexer to be excited in-phase respectively with SHLD1 or SHLD2. These two shield pins are shorted to each other in single-ended measurement mode (chanel to ground) when chanel CHB is disabled and CAPDAC section can be used for capacitance offset of each input chanel. In differential measurement mode of the FDC1004, CAPDAC is unable and the shield pins are driven out of phase with each other. It needs to be noticed that the index of the input chanel selected to chanel CHA must be less than that of which selected to chanel CHB. The input chanel in CHA or CHB is subsequently forwarded to the CDC section of the FDC1004 (see Figure 15). [8.]

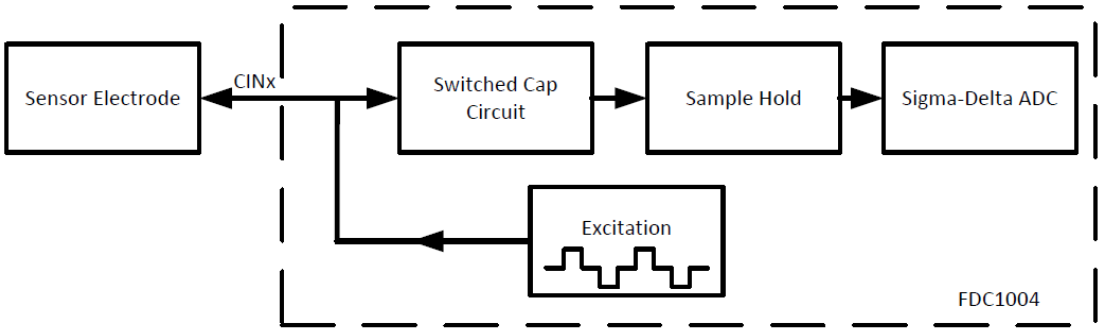

Figure 15. Capacitance to digital conversion theory of FDC1004 [1, 4]

The CDC implements a switched capacitor circuit to transfer charge from the sensor electrode to the sigma-delta analog to digital converter (ADC). The sensor electrode is previously charged up by an excitation of a 25 kHz step waveform for a particular duration of time. The charge on the electrode is then transferred to a sample-hold circuit after another certain amount of time. The analog voltage is derived out and converted into a digital signal by the sigma-delta ADC. Once the conversion is completed, the result is digitally filtered and corrected by gain and offset calibrations. Selecting of input channels, configuring measurement modes, activating the CDC and Gain-Offset section, and reading measurement results are executed on I^2C interface which allows a master MCU access the configuration and data registers of the FDC1004 and transfer data between them. [1, 4.]

2.4 I^2C data transfer between MCU and FDC1004

I^2C serial communication interface between integrated circuits (ICs) was developed by the Philips semiconductor division (now NXP). An I^2C interface consists of two data wires, known as serial data (SDA) and serial clock (SCL). They are connected through pull-up resistors to the power supply voltage (Vcc) and a common voltage reference (GND) is shared by ICs on the bus (see Figure 16).

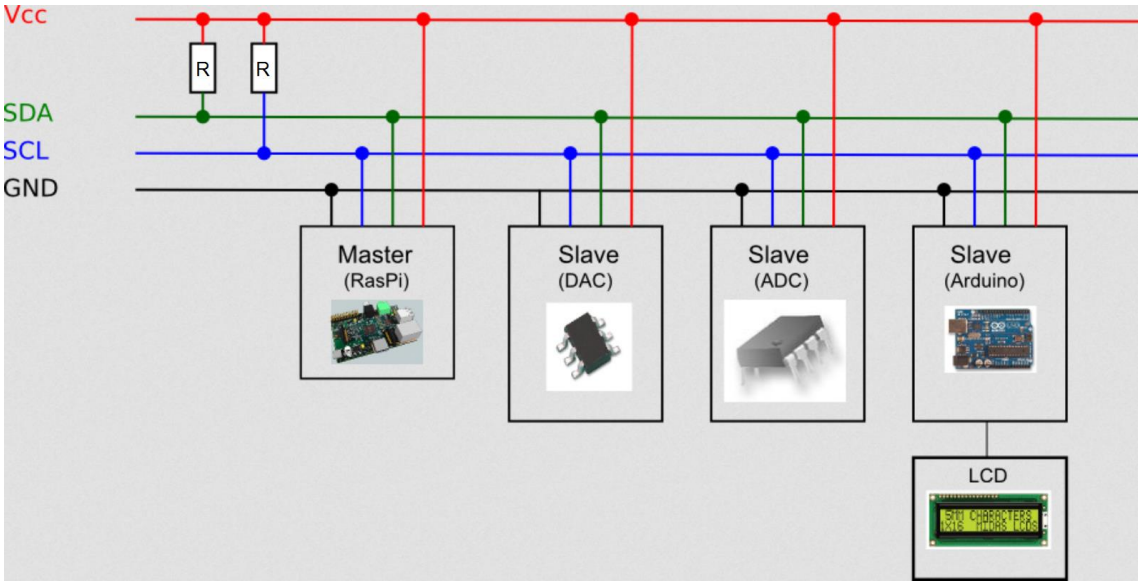

Figure 16. Diagram of a typical I²C configuration [10]

I²C interface allows a master device to communicate with slave devices on the same bus. An I²C master is the device that generates clock, initiates communication, sends I²C commands and stops communication on the bus. An I²C slave is the device that listens to the bus and is addressed by the master. Each slave on the bus must have a unique address to be detected by the master. If there are more than one master and each requires the bus, an arbitration process takes place to determine which of the masters on the bus can use it. The masters which have lost arbitration must release the bus and go into slave mode. [11.]

The master generates clock pulses on SCL wire. For each clock pulse one bit of data is transferred on SDA wire. Each I²C command is initiated by the master with a START condition and ends with a STOP condition. While SCL must be high, START condition is detected with a high to low transition of SDA signal and STOP condition with a low to high transition. After a Start condition, the bus is considered as busy and rejects other master devices requesting it until a Stop condition is detected. During I²C command, data is transferred on SDC wire in a number of bytes. All the bytes are transferred with each most significant bit (MSB) shifted first. Each byte must be followed by an Acknowledge (ACK) bit by the slave. This bit is set low if the slave is ready for the transfer of the next byte. [11.]

The FDC1004 operates as a slave device which has a unique 7-bit I²C address on the two-wire bus interface. The master initiates communication on the I²C bus with Start

condition, followed by the 7-bit slave address and the data direction (R/$\overline{W}$) bit. If this bit is 0 then the master will transmit data to the slave device (write operation). Otherwise, if the data direction bit is set to 1, the master will receive data from slave device (read operation). After the slave address and the data direction is sent, the slave is detected and acknowledges the transfer and then the master can continue with reading or writing on the bus until a Stop condition is detected. Figure 17 illustrates write frame of data transfer on the I^{2}C bus between a master and a 7-bit I^{2}C address slave. The slave has a pointer register. The value of the pointer is the address of a data register of the slave. After the slave's first acknowledgement of the transfer in write mode, the master writes the data register address to the pointer and data bytes are then written into the corresponding data register. [8, 13-14.]

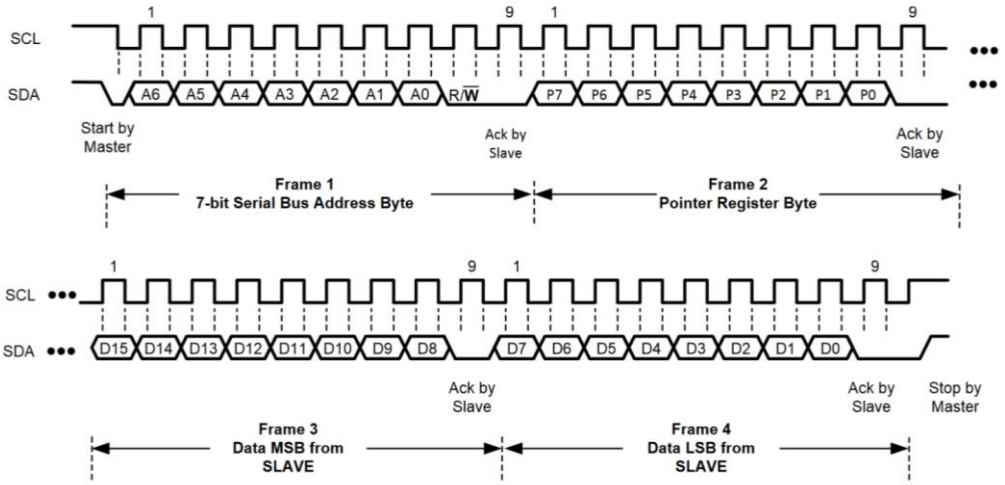

Figure 17. Write frame on I^{2}C bus [8, 14]

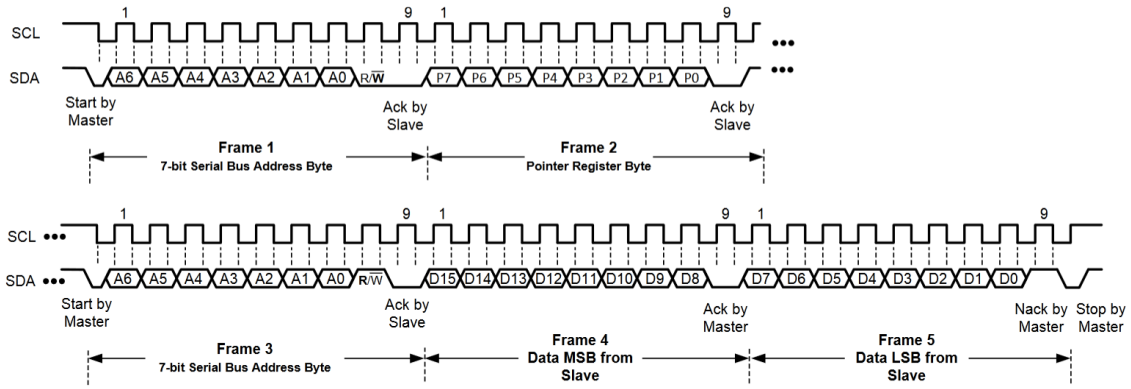

Figure 18. Read frame on I^{2}C bus [8, 14]

Figure 18 explains read operation on the I^2C bus [8, 14]. To read the data stored in a data register of the slave, the address of that data register is written to the pointer by in a write operation. However, the master won't write the data to the data register and turns to change the data transfer direction from write mode to read mode by resending the slave address bit and resetting the data direction bit to 1. After the slave acknowledges to start read mode, the data from the desired data register of the slave is transferred onto the bus and received by the master.

3 Methods and Materials

The theoretical analysis in this document bases on literature primarily from online sources. A model of the coplanar-plate capacitor was simulated by COMSOL Multiphysics software to illustrate the two dimension electric field by the capacitor model. This software applies graphical user interface (GUI) with powerful modelling tools for simulation of different designs in electrical, mechanical, fluid flow, and chemical applications. Other theoretically analysing graphs were made by Excel Microsoft.

In implementation of designing the sensor for liquid level application, PADS Layout is the CAD program used to produce the flexible printed circuit (FPC) layout of a sensor port and a small zip connector board needed for connection between the sensor and the FDC1004 on a mini test board for a single measurement setup. After the design of the sensor port had been completed, an order was sent to the printed circuit board (PCB) manufacturer Prinel for prototyping. CircuitCAM software, milling machine and lab tools (multimeter, solder iron etc.) were needed for milling the zip connector board, soldering and electrical testing.

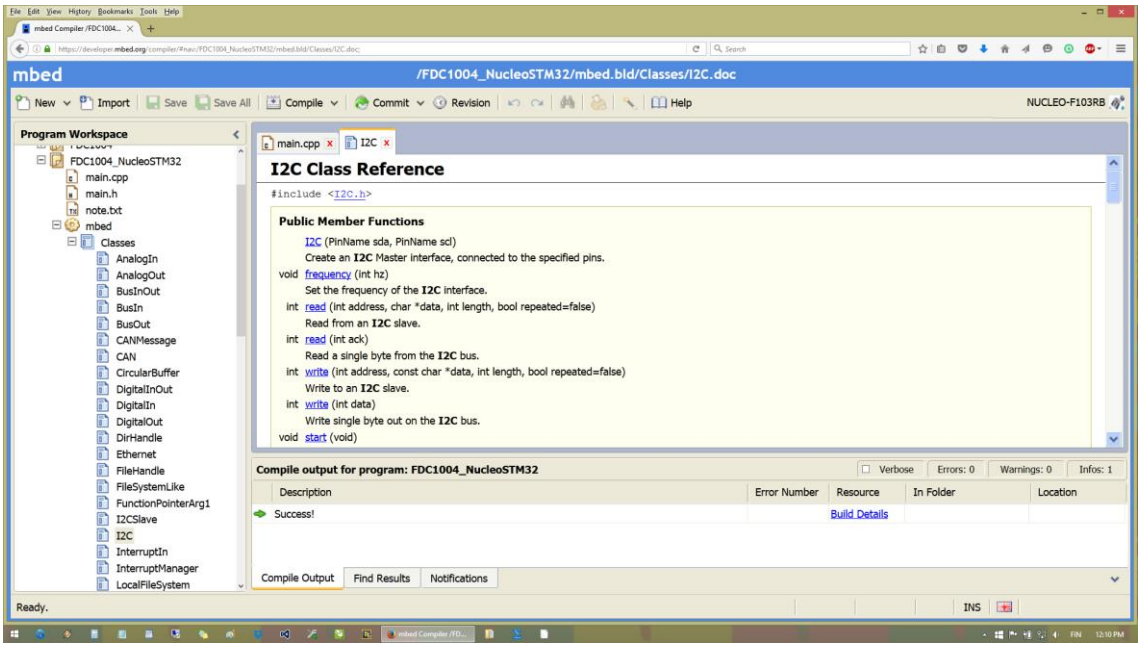

Figure 19. Online compiler IDE on ARM mbed developer site.

For programming, the online mbed compiler is an integrated development environment (IDE) friendly and popularly used on ARM mbed developer site. To set up measurements for liquid level application with the FDC1004, most MCUs supported with I^2C interface can be used as a master device. The online mbed compiler IDE supports various MCU hardware platforms to ease prototyping using the target MCU with an official mbed C/C++ software development kit (SDK). The SDK provides the software platform and libraries to build a program or an application to be run on the selected MCU platform. Figure 19 shows the online mbed IDE interface and the mbed built-in library which provides I^2C class reference to build a target application. In available and convenient conditions of this project, the Nucleo-F103RB platform was selected to build an application for testing the sensor with the FDC1004. The Nucleo platform is one of products of the electronics and semiconductor manufacturer STMicroelectronics for quick prototyping of the target STM-MCUs. Therefore, ST link driver and firmware needed installation to a personal computer (PC) for compiling the test code into the STM32 MCU via a universal serial bus (USB). Figure 19 represents the pinout of the Nucleo-STM32 which will be referred to use serial transmitter and receiver, I^2C and digital pins for the application. Measurement results are read via the same USB serial port on Tera Term serial terminal which is already installed on the PC. The transmission between the devices is described in details for the measurement setup in section 6.

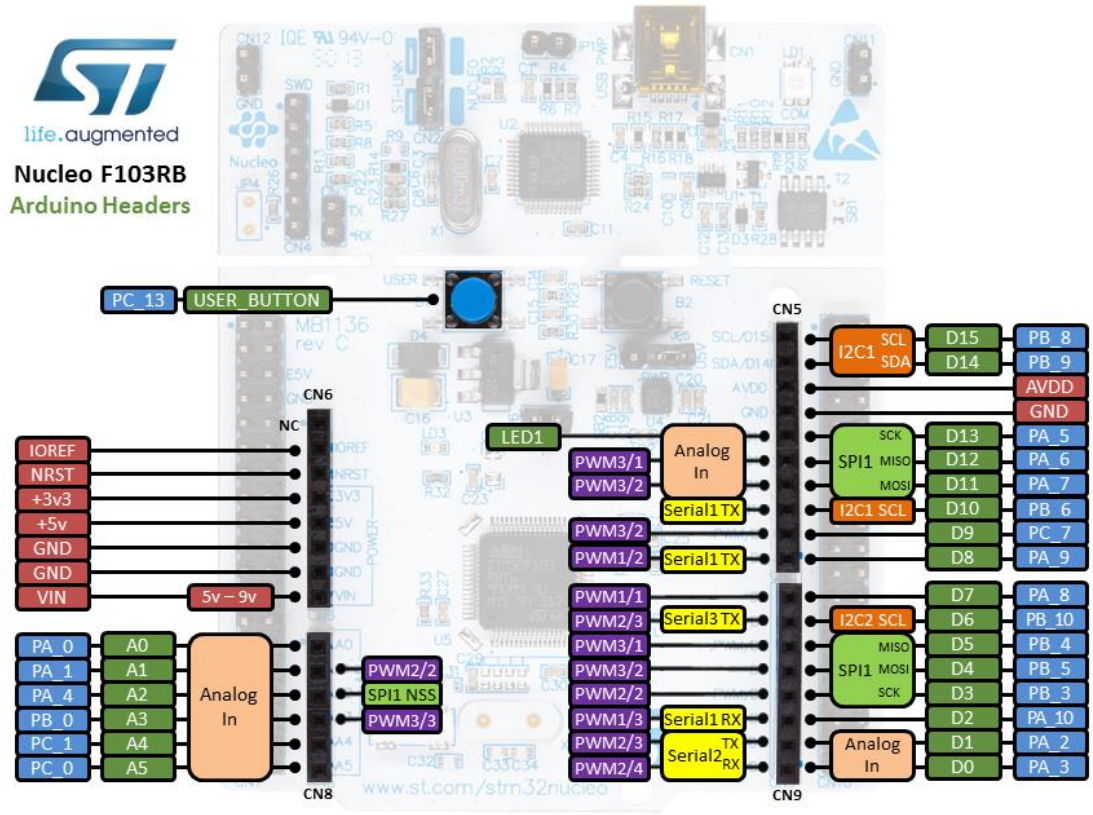

Figure 20. Nucleo-F103RB pinout

4 Sensor Layout Design

The sensor electrodes have designed with geometrical parameters selected for a sufficient sensitivity. In the backflow prevention device prototype, the water cylindrical tank of 100mm radius and 50mm height limits a measurement space of the water level sensor. There is a height limit of the sensor to be designed at maximum 45mm. Therefore, three sensor electrode pairs have the same 18um thickness, 6mm width and 2mm separation but the different heights: 45mm for LEVEL sensor, 10mm for Reference sensors. Since each electrode is seen at a small angle of around 7 degree along the radius by the axis when bended along the circular length of the cylindrical tank, it is estimated acting the same way as the coplanar model. The field penetration depth of each sensor can be estimated by Equation 16:

$$T = \frac{a}{2}\sqrt{\left(1+\frac{2w}{a}\right)^2 - 1} \approx \frac{2}{2}\sqrt{\left(1+\frac{2\times 6}{2}\right)^2 - 1} \approx 7\text{mm}$$

Thus, water space in the tank should be large enough (about 100mm thickness seen by the sensor) for the sensor to work according to the model. In the other words, the sensor capacitance should be proportional to the water level in the tank and OoP liquid level differential measurement can be applied for water level sensing.

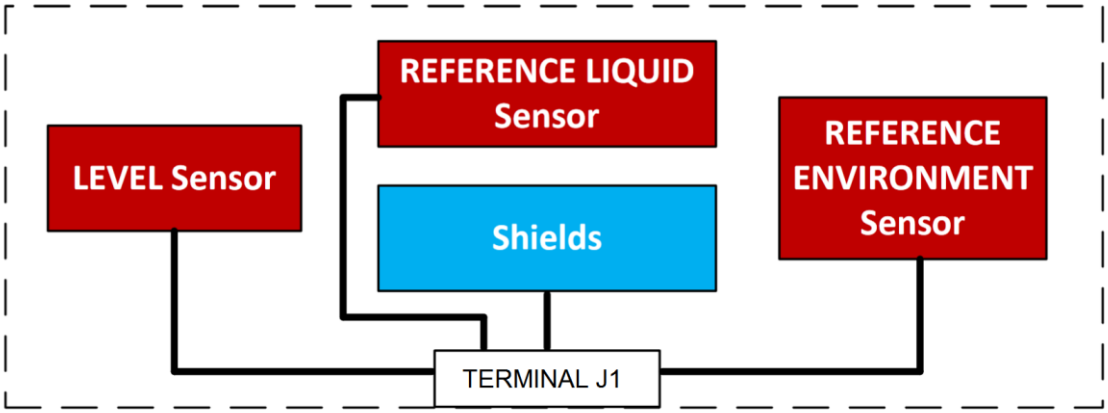

Figure 21. Design block diagram of the liquid level FPC sensor port [6, 1]

The sensor port is designed as a FPC board of two 18um-thick-copper layers on which the sensor and shield electrodes are printed and traced to a terminal (see Figures 21). The terminal J1 is required being connected to the FDC1004 via a zip flat flexible cable (FFC) connector on the control board of the backflow prevention device. Therefore, the sensor terminal is of the kind which fits zip FFC connector with the following parameters: 1mm-wide pitch between adjacent pins of 0.6mm width and at least 4mm length. The 10-pin terminal and the zip connector are contacted from bottom side. Each pin of the zip connector is matched to a corresponding FDC1004 input pin as showed in Figure 22.

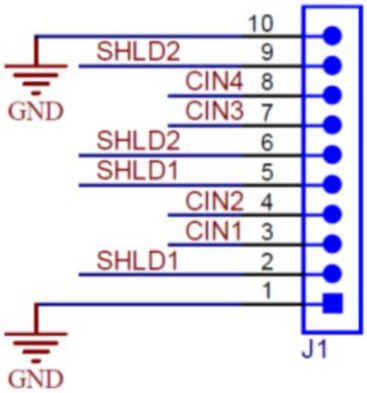

Figure 22. Schematic of sensor connection to FDC1004 [6, 17]

The LEVEL sensor includes the LEVEL electrode and its paired electrode. The LEVEL electrode and its shield are connected to CIN1 and SHLD1 pin. The electrode paired with LEVEL electrode and its shield are connected to the same SHLD2 pin. The RL and RE sensor have the similar connection to FDC1004 pins as the LEVEL sensor, except the RL electrode jointed to CIN2 pin and the RE electrode to CIN3 pin. The sensor port has no connection to CIN4 and GND pins.

Three sensors on the bottom side of a base polyimide layer each include a pair of (bottom copper) electrodes whose (top copper) shields are on the top side. The thickness of the FPC and of each layer are estimated as in Figure 23. The terminal region is supported by a stiffener and all vias between the copper layers are collected at this rigid area beside terminal pins. The traces between electrodes and terminal pins should be round at corners for least broken risk thereof.

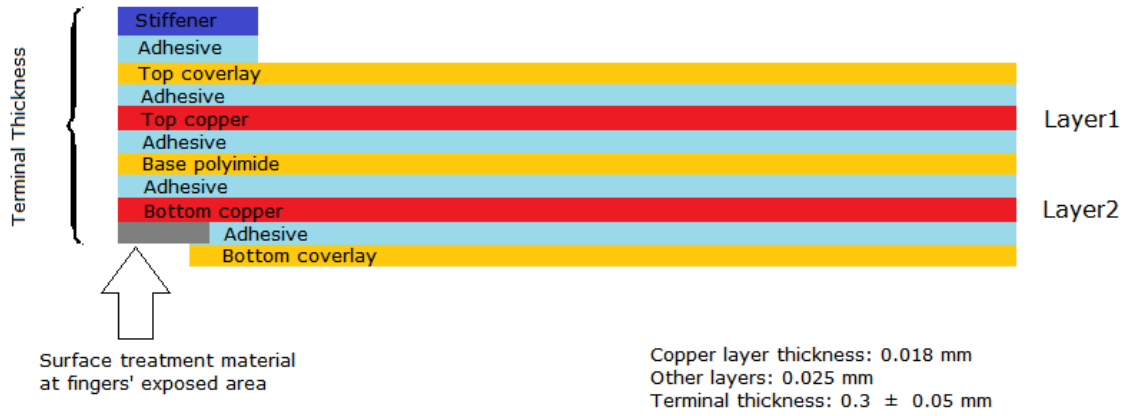

Figure 23. Stack-up of two layer FPC terminated with zip contact fingers.

Collecting all specifications, the sensor port layout have designed by PADS Layout program. Figures 24 – 30 show the top view construction of each layer. Arrangement and positon of electrodes and shields relative to each other must be the way to ensure the highest symmetry of the system.

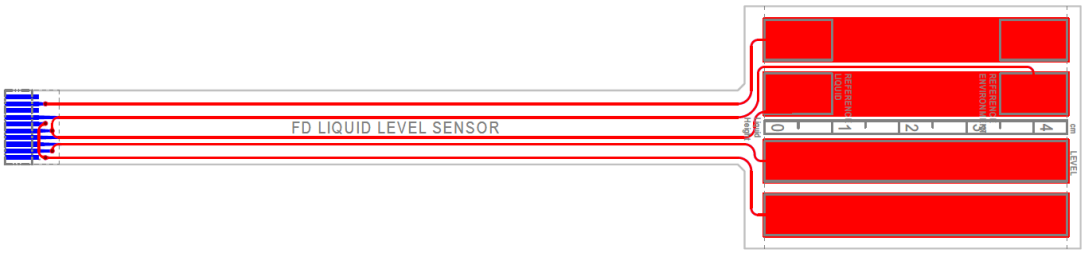

Figure 24. Composite view

Figure 25. Stiffener layer

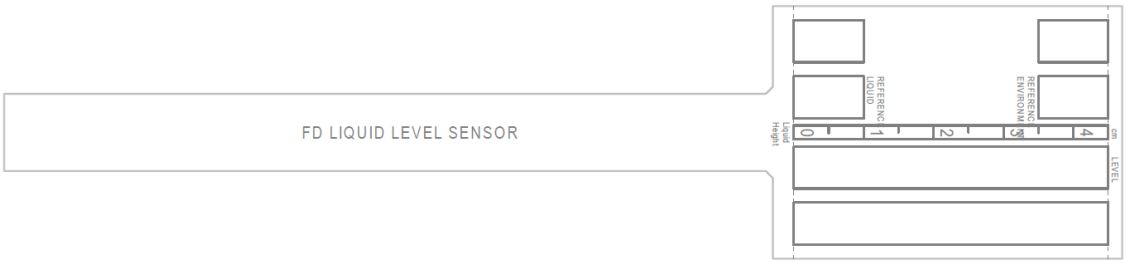

Figure 26. Silkscreen top

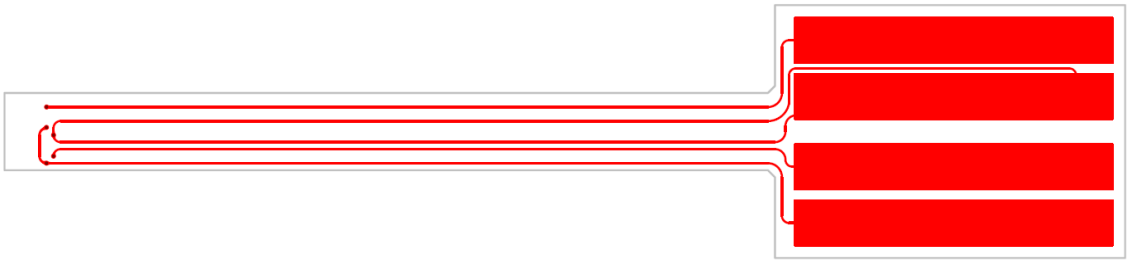

Figure 27. Top copper layer

Figure 28. Base polyimide layer and drill drawing

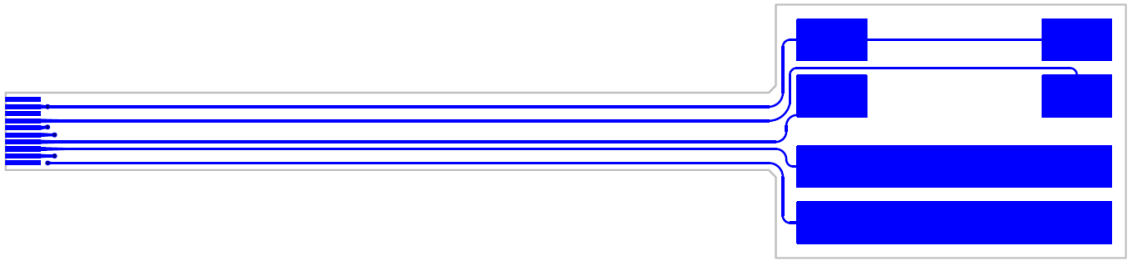

Figure 29. Bottom copper layer

Figure 30. Dimension of the sensor port

5 Programming

To program the STM32 MCU on the Nucleo platform for testing the liquid level sensor prototype, there is a need to use the official mbed built-in library in the online mbed compiler IDE. Therefore, it is required to always include the *mbed.h* header file first in the code (see Appendix 1 and 2). The library provides source codes constructing classes I^2C and Serial which support to set up an I^2C master interface of the MCU and an "USB virtual serial port" for printing out messages to the host PC terminal [12]. LED1 pin of the Nucleo-F103RB is also used as a digital output for checking any transmission error

between the MCU and the FDC1004. These I^2C, serial and digital output pins are declared as in Listing 1.

```
#include "mbed.h"
I2C i2c(I2C_SDA, I2C_SCL);
DigitalOut myled(LED1);
Serial pc(SERIAL_TX, SERIAL_RX);
```

Listing 1. Inclusion of *mbed.h* header file and creation of objects for I^2C, serial interfaces and digital output pin.

Next starts configuring the FDC1004 for three measurements of LEVEL, RL and RE sensor capacitances and figures out the material to write essential function calls for I^2C commands between the MCU and the FDC1004. To measure the LEVEL sensor, all features related to measurement 1 setup are taken into account. From the datasheet of the FDC1004, the registers in the major duty to measurement 1 include:

- MEAS1_MSB and MEAS1_LSB (to be read only the MSB and LSB portion of the measurement 1 result),
- CONF_MEAS1 (to select the corresponding input channels into CHA and CHB channel and to adjust the CAPDAC value for an offset capacitance if enabled),
- FDC_CONF (to select reset/non-reset mode, sample rate at 100Hz/200HZ/ 300H/400Hz, single/repeated mode, trigger/finish of measurement 1)

The LEVEL sensor capacitance is measured between CIN1 and SHLD2 pin to which two electrodes of the LEVEL sensor connected. Therefore, CONF_MEAS1 must be set to 0x0C00 so that CIN1 into CHA and CIN4 into CHB and zero CAPDAC. Meanwhile FDC_CONF is set to 0x0C80 for measurement 1 to be non-reset, sampled at 400Hz and trigged single time. In non-repeated mode FDC_CONF must be re-written each time for a new single measurement, that means each configured measurement must be performed after another has been done. In the similar consideration of measurement features, configuration of a single measurement of each sensor at each starting is collected in Table 1.

Table 1. Configuration of a single measurement at each starting

Configuration of single measurement at each starting	Pointer	Register Name	Value
Measurement 1 (LEVEL)	0x00	MEAS1_MSB	0x0000
	0x01	MEAS1_LSB	0x0000
	0x08	CONF_MEAS1	0x0C00
	0x0C	FDC_CONF	0x0C80
Measurement 2 (RL)	0x02	MEAS2_MSB	0x0000
	0x03	MEAS2_LSB	0x0000
	0x09	CONF_MEAS2	0x2C00
	0x0C	FDC_CONF	0x0C40
Measurement 3 (RE)	0x04	MEAS3_MSB	0x0000
	0x05	MEAS3_LSB	0x0000
	0x0A	CONF_MEAS3	0x4C00
	0x0C	FDC_CONF	0x0C20

Hence arises the first requirement to use function calls of *i2c.write and i2c.read* from the mbed library to create I^2C commands between the master and the slave. For the purpose to configure the registers CONF_MEASx and FDC_CONF and read the measurement result from the data registers MEASx_MSB and MEASx_LSB correspondingly of each measurement, two functions are declared as in Listing 2.

```
static void Config(char pointer, char msb, char lsb)
static int Read_Meas(char MEAS_MSB, char MEAS_LSB)
```

Listing 2. Functions for configuring and reading measurements.

The *Config* function is intended to use *i2c.write* library function to write the MSB byte “msb” first and the LSB byte “lsb” later into the data register that the “pointer” point to. If there is any transmission error in this stage of the FDC1004 configuration, then the measurement fails to be active. So the LED1 of the Nucleo MCU board does its duty here to alarm the error by toggling faster (every 0.2 second for example) than the normal speed (every 1 second). Whereas, the *Read_Meas* function must use in addition of *i2c.read* library function call to read the MSB and LSB portions of the measurement result

from the two specified data registers. In the other words, the *Read_Meas* function is simply calling twice a function to read each 16-bit register of the slave and combining the results into a 32-bit memory register of the MCU. It should be noticed that the measurement result is given by the FDC1004 in a signed 24-bit integer of Two's Complement. However, a call of the *Read_Meas* function is producing otherwise a signed 32-bit integer of Two's Complement. Therefore, a translation is needed for the result of capacitance to be displayed in the end.

The function to read a single register of the FDC1004 can be apparently named as:

```
static int Read_1_register(char pointer)
```

in which the "pointer" is the address of the register desired to be read. The average time for each measurement sample to be done is 1/400Hz = 2.5ms, i.e. about 3ms after a trigger of measurement 1 FDC_CONF automatically turns to 0x0C81. This can be easily checked by a *pc.printf* operation for printing to the PC terminal the return from a call of the *Read_1_register* function to read FDC_CONF after a *wait(0.003)*. The *pc.printf* operation is also used to display the measurement results on the PC terminal.

Figure 31 refers to write and read function of I^2C class in the mbed library [13]. As required previously, the *Config* function can be defined with a call of the i2c.write function with parameters: the 8-bit I^2C slave address of the FDC1004; the pointer to a byte-data array of 3 bytes "pointer", "msb", "lsb" to be transmitted; and a stop to end the write command. If there is a return of non-0 with no acknowledgement by the slave, the LED1 will be toggle every 0.2 second. The FDC1004 has an 8-bit I^2C slave address that is 0xA0 including 7-bit slave address bit[7:1] and the data direction bit[0] at 0 as default and indicating a write mode.

int write (int *address*,
const char * *data*,
int *length*,
bool *repeated* = `false`
)

Write to an **I2C** slave.

Performs a complete write transaction. The bottom bit of the address is forced to 0 to indicate a write.

Parameters:

address	8-bit **I2C** slave address [addr | 0]
data	Pointer to the byte-array data to send
length	Number of bytes to send
repeated	Repeated start, true - do not send stop at end

Returns:

0 on success (ack), non-0 on failure (nack)

int read (int *address*,
char * *data*,
int *length*,
bool *repeated* = `false`
)

Read from an **I2C** slave.

Performs a complete read transaction. The bottom bit of the address is forced to 1 to indicate a read.

Parameters:

address	8-bit **I2C** slave address [addr | 1]
data	Pointer to the byte-array to read data in to
length	Number of bytes to read
repeated	Repeated start, true - don't send stop at end

Returns:

0 on success (ack), non-0 on failure (nack)

Figure 31. Write and read function of I²C class reference in the mbed library

The *Read_1_register* function can be defined as a combinative I²C command of an I²C write with no stop and an I²C read with a stop. First the I²C writes the “pointer” after the 8-bit FDC1004 address and no stop. Next a call of the *i2c.read* function will reset the data direction bit[0] to 1. Finally, the I²C read 2 data bytes (always MSB byte first) of the register which the “pointer” points to, transfer the data to the MCU and stop the read transaction. The *Read_Meas* function can be simply defined by providing the corresponding addresses of MEASx_MSB and MEASx_LSB registers to each call of *Read_1_register* function reading one of these register. The 24-bit measurement result translated into a 32-bit sized data.

The address, configuration and data registers of the FDC1004 and the *Config, Read_1_register* and *Read_Meas* function can be defined separately in a *main.h* header file to be included in the main code. In the main code, a slight control logic and calculation of capacitances and liquid level has been built with the defined functions. Noticed that measurements in differential mode of the FDC1004 has no offset capacitance contribution to the measurement result, the capacitance is calculated as:

$$\text{Capacitance}\left(\text{pf}\right) = \left(\left(\text{Two's Complement}\left(\text{measurement}\left[23:0\right]\right)\right) / 2^{19}\right) \quad (32)$$

Equations 30 and 31 are applied to derive the water level to be measured with or without the use of the RE sensor as shown in Listing 3.

```
ratio = (cap1 – level0)/(cap2 – ref0)
level = (cap1 – level0)/(cap2 – cap3)
```

Listing 3. Calculation of the water level measured with and without the RE sensor concerned.

6 Measurement and Calibration

6.1 Measurement Setup

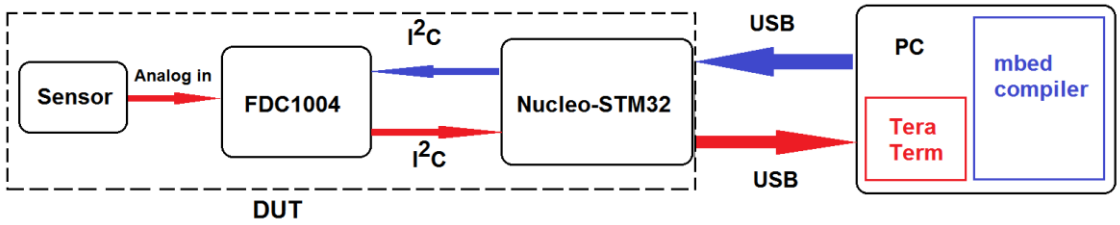

Figure 32. Measurement setup of the liquid level system

The measurement system of the liquid level OoP technique includes 4 sections as described in Figure 32. The devices under test (DUT) are shown in Figure 33. Figure 34-36 shows the implementation process of the measurement. The PC is connected to the internet and opened with two programs: the online mbed compiler and Tera Terminal. The PC communicates with the STM32F103RB microcontroller of Nucleo-F103RB platform via the ST link USB interface. The test code is compiled to the MCU by the mbed compiler and the data from the MCU is then received and displayed in Tera Term window at COM6 serial port. The FDC1004 is separated on a mini test board using two

1k8 pull-up resistors between SCL and SDA pins and 3.3V power line from the MCU. The MCU talks to the FDC1004 about the sensor on the I^2C bus. The sensor port pasted to the outside of a nonconductive bottom is connected to the FDC1004 via a zip connector on another small separate board as mentioned previously. The measurement results are read at different heights of the water column in the bottom: zero level with the bottom empty, 10mm (the same height of the RL sensor), 15mm, 20mm … The level is measured at maximum 35 mm with or 45mm without the reference of RE sensor.

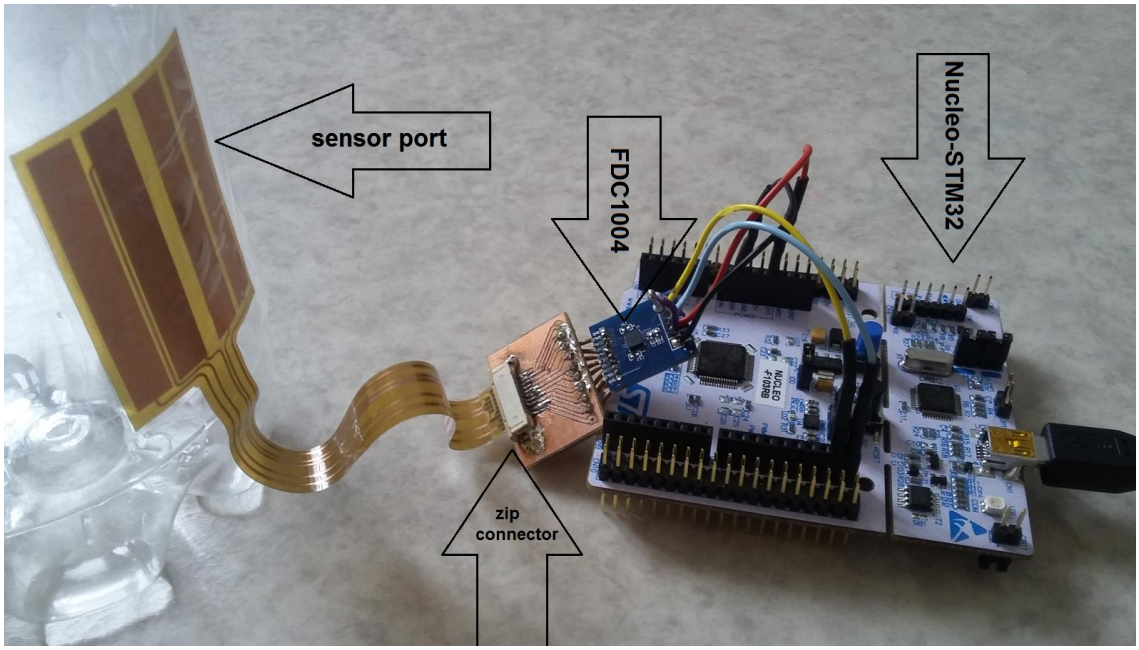

Figure 33. Devices under test

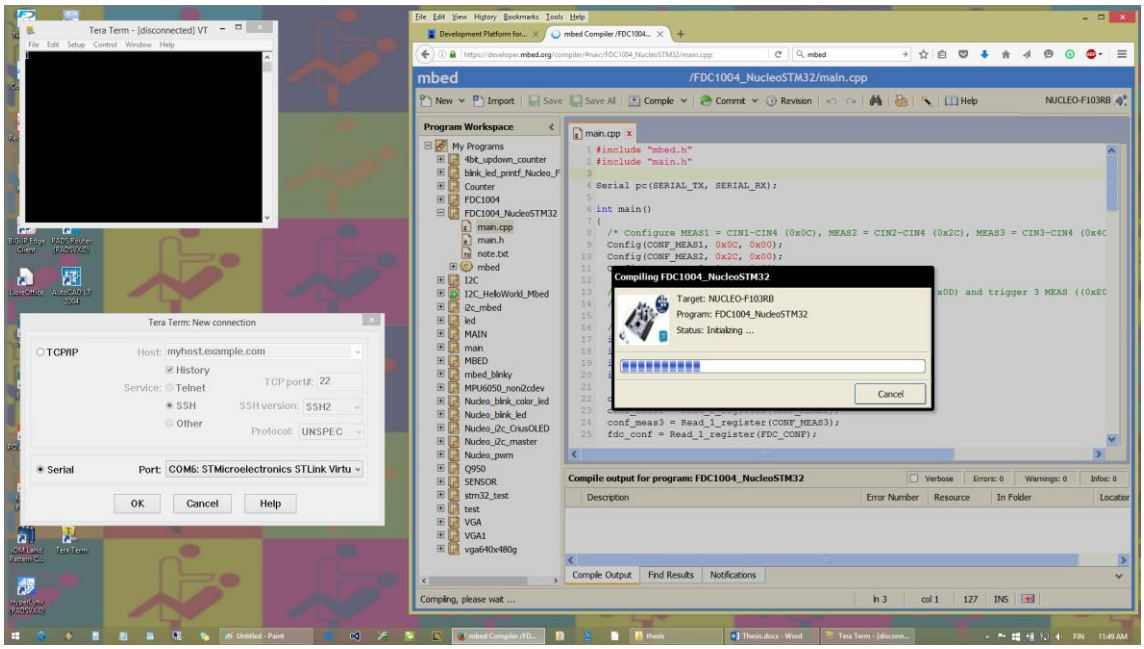

Figure 34. Tera Term display at COM6 serial port and the test code compiled to the MCU

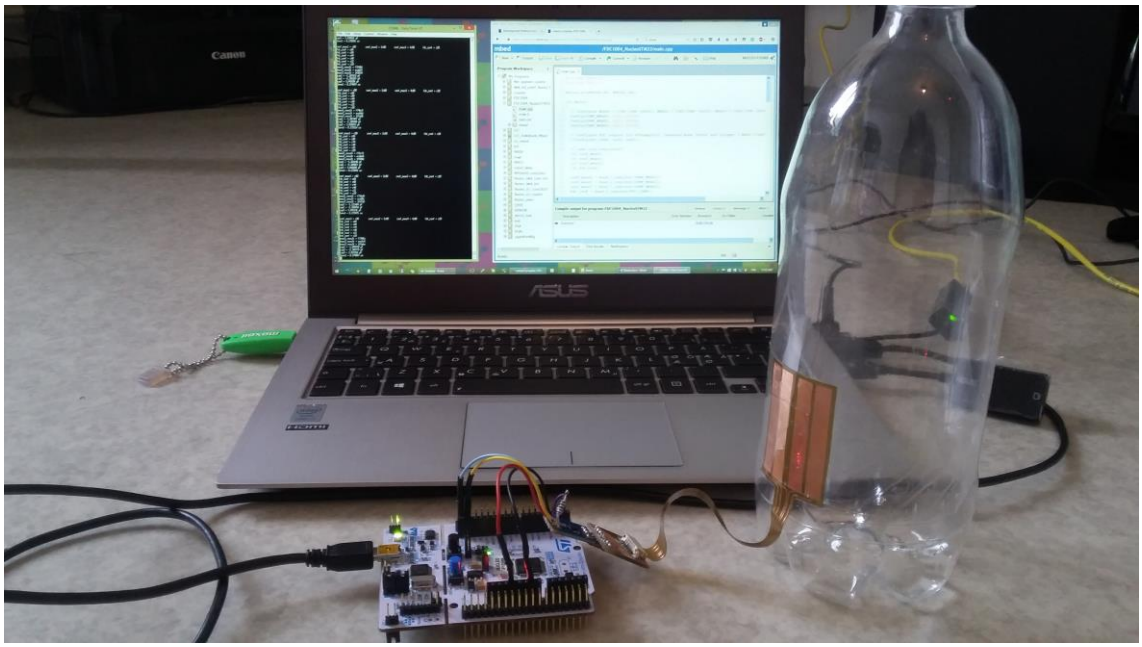

Figure 35. Testing

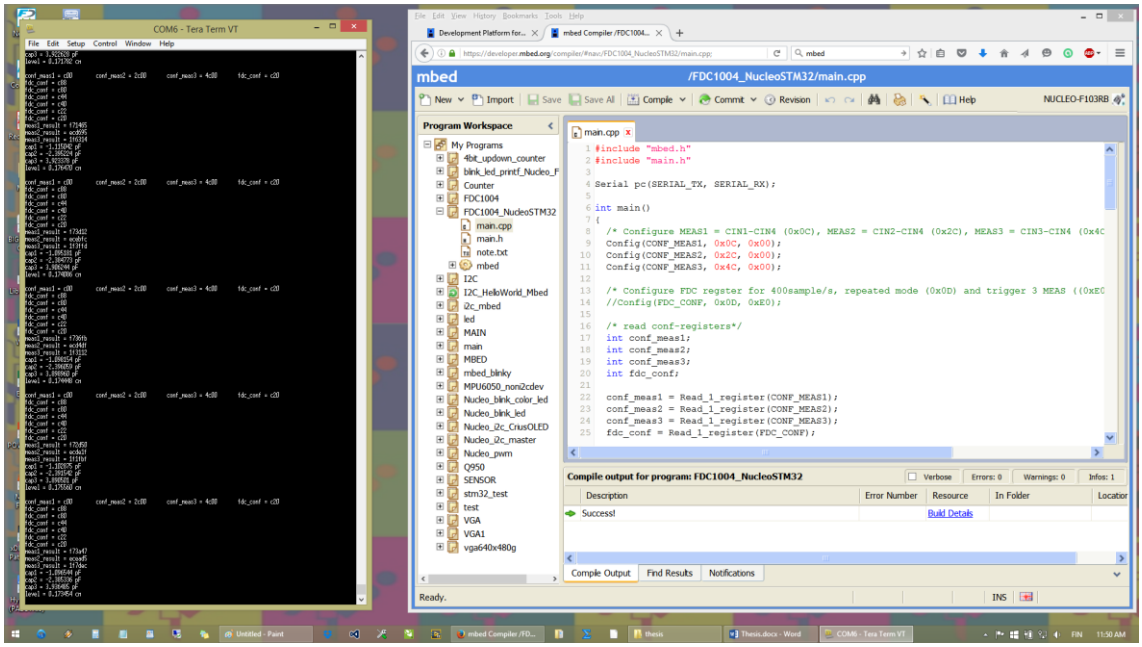

Figure 36. Measurement results read from Tera Terminal

Another test code with the same configuration for sensor-FDC1004-MCU data transfer was written for the control board of the backflow prevention prototype. An application program interface (API) was written by a Finndent software engineer on a different IDE for the target MCU, which is refused to be reported in details due to the limit of this document. However, the same measurement process of different water levels were

performed and the results are analysed and discussed in a later section. Figure 37 simply shows the measurement setup as a part of the evidence of implementation of the project.

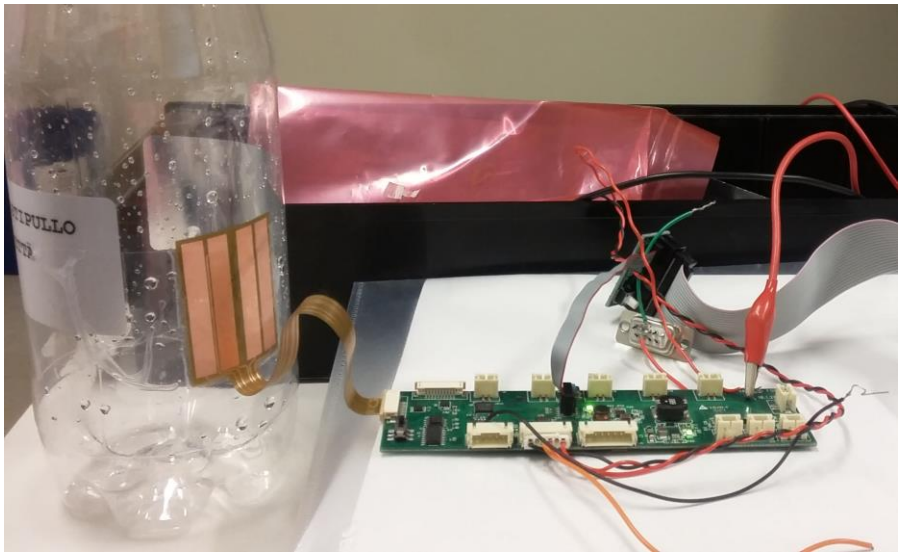

Figure 37. Measurement setup with the backflow control board

6.2 Calibration of Measurement

The measured level can be linearly varying compared to the actual liquid level. This is possible due to inequivalent variations in the LEVEL, RL and RE electrode capacitances for each liquid level interval. A first linear correction algorithm can be applied to compensation for the variations:

$$\text{level}' = \text{gain} \cdot \text{level} + \text{offset} \tag{33}$$

[6, 8.]

7 Results and Discussion

7.1 Measurement with Nucleo-STM32

Table 2. Measurement result of capacitances with the Nucleo-STM32

Actual level	Capacitances (pF)	Value 1	Value 2	Value 3	Value 4	Value 5	Rounded Value
0 cm	LEVEL	-0.920	-0.930	-0.902	-0.930	-0.948	-0.9
	RL	-2.413	-2.419	-2.392	-2.413	-2.405	-2.4
	RE	4.109	4.124	4.115	4.119	4.090	4.1
1 cm	LEVEL	0.073	0.107	0.015	0.069	0.078	0.1
	RL	-2.381	-2.388	-2.385	-2.389	-2.388	-2.4
	RE	4.378	4.350	4.400	4.377	4.373	4.4
1.5cm	LEVEL	0.303	0.325	0.367	0.338	0.244	0.3
	RL	-2.358	-2.367	-2.349	-2.367	-2.360	-2.4
	RE	4.387	4.423	4.394	4.390	4.386	4.4
2 cm	LEVEL	0.636	0.611	0.712	0.662	0.641	0.6
	RL	-2.360	-2.363	-2.374	-2.378	-2.400	-2.4
	RE	4.449	4.459	4.434	4.414	4.365	4.4
2.5cm	LEVEL	1.014	1.051	1.064	1.013	1.071	1.1
	RL	-2.377	-2.363	-2.363	-2.357	-2.337	-2.4
	RE	4.483	4.390	4.450	4.541	4.463	4.5
3 cm	LEVEL	1.544	1.639	1.623	1.533	1.583	1.5
	RL	-2.343	-2.373	-2.339	-2.337	-2.366	-2.4
	RE	4.505	4.571	4.641	4.514	4.549	4.5
3.5cm	LEVEL	2.309	2.224	2.253	2.291	2.275	2.3
	RL	-2.335	-2.346	-2.356	-2.345	-2.381	-2.3
	RE	4.611	4.630	4.595	4.646	4.670	4.6
4cm	LEVEL	3.168	3.240	3.242	3.311	3.316	3.2
	RL	-2.354	-2.337	-2.340	-2.340	-2.340	-2.3
	RE	5.568	5.658	5.613	5.678	5.656	5.6
4.5cm	LEVEL	4.327	4.394	4.399	4.319	4.342	4.3
	RL	-2.296	-2.315	-2.305	-2.284	-2.320	-2.3
	RE	6.760	6.771	6.754	6.802	6.751	6.8

NOTE: level0 = -0.9, ref0 = -2.4

Unfortunately, the capacitance measurement result with the Nucleo-STM32 is seriously unreliable. Five measured capacitance values of each sensor were read directly from the Tera Terminal and collected in Table 2. It is still a mystery with negative values of LEVEL and RL capacitances although the FDC1004 measures a capacitance difference between two input channels and can produces a negative value thereof. They were expected to be positive as well as RL and RE capacitances should be approximate to each other at zero level as the bottom is empty. The only trusty possibility is that the LEVEL capacitance increases due to the increasing actual level of the water in the bottom. The RL capacitance nearly remained stable over time but it should have jumped dramatically according to a jump from 0 to 1cm of the water level. In contrast, the RE showed a proper behaviour as expected and an impressive rise since the water level climbed over 3.5 cm height but its value was even higher than the LEVEL's. It can be guessed the origin of the problem from the parasitic capacitance of poor connection between the sensor port and the FDC1004 mini board via the zip connector board. Long and bad connection path from the sensor to FDC1004 through these PCBs causes significant parasitic capacitance not eliminated by proper shielding.

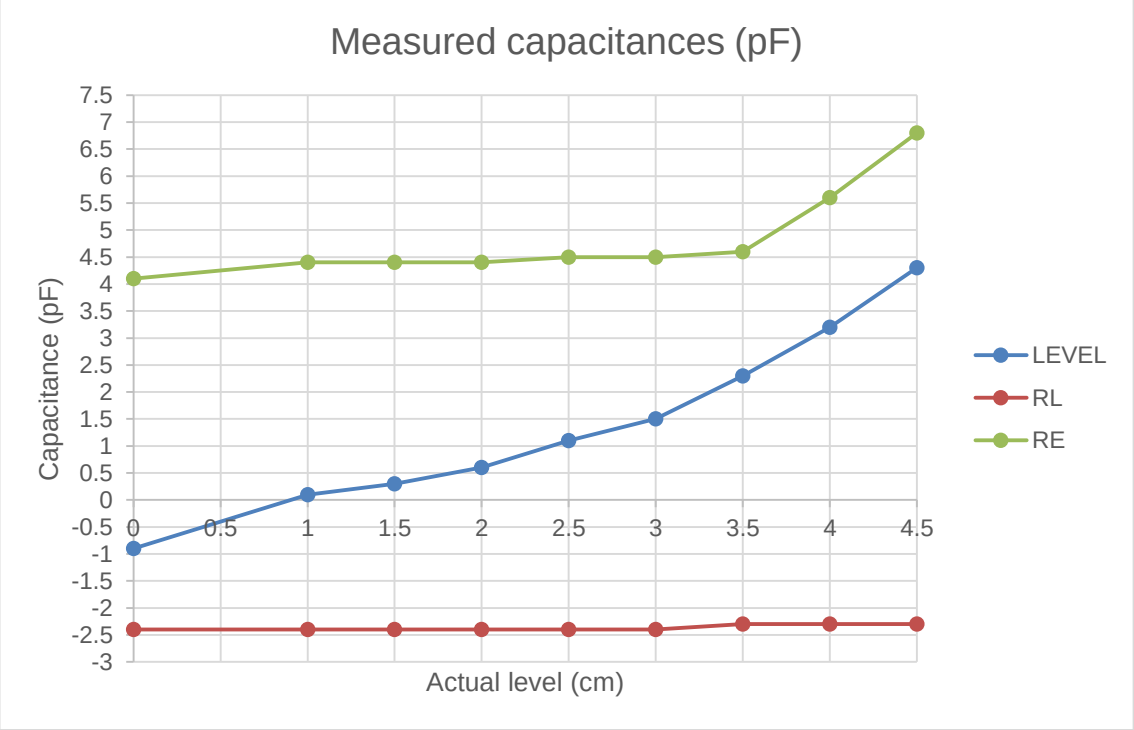

Figure 38. Capacitance measurement results with the Nucleo-STM32.

The suggestion for a solution to the parasitic capacitance is to design the FDC1004 on the same flex-rigid PCB of the sensor for as minimal connection length as possible. However, the reaction of the RL sensor in this setup is still in a difficult question to be answered. Figure 38 indicates the LEVEL showing its rapid change when the water level reach the lower edge of the RE sensor. There occurs a doubt that SHLD2 electrode capacitance changing due to the water level affected the LEVEL capacitance measurement in the vicinity of the RE sensor. It is noticed that shield signal pins are continuously connected over time. Meanwhile, only one (CINx) sensor electrode is connected each time in its turn of measurement; otherwise, it is floating. Nevertheless, if this change is actually linear as can be seen from 3.5cm to 4.5cm then the level can be calibrated with appropriate gains and offsets for different linear segments. This method can be applied to better treat the results of capacitance measurement with the backflow control board where the FDC1004 was designed as close to the sensor as possible.

7.2 Measurement with Backflow Control Board

Table 3. Measurement result of capacitances with the backflow control board

Actual level	Capacitances (pF)	1	2	3	4	5	round
0 cm	LEVEL	1.776	1.779	1.774	1.771	1.771	1.8
	RL	0.377	0.373	0.372	0.374	0.372	0.4
	RE	2.975	2.970	2.971	2.985	2.979	3.0
1 cm	LEVEL	2.495	2.493	2.497	2.506	2.497	2.5
	RL	1.158	1.168	1.160	1.174	1.168	1.2
	RE	3.206	3.202	3.210	3.216	3.202	3.2
	ratio	0.943	0.929	0.944	0.938	0.934	0.9
1.5 cm	LEVEL	2.720	2.711	2.716	2.726	2.712	2.7
	RL	1.182	1.188	1.187	1.185	1.176	1.2
	RE	3.211	3.219	3.219	3.223	3.238	3.2
	ratio	1.202	1.182	1.190	1.205	1.202	1.2
2 cm	LEVEL	3.028	3.040	3.043	3.034	3.013	3.0
	RL	1.191	1.200	1.193	1.205	1.192	1.2
	RE	3.258	3.259	3.260	3.249	3.260	3.3
	ratio	1.577	1.577	1.593	1.557	1.555	1.6

2.5cm	LEVEL	3.489	3.519	3.509	3.517	3.525	3.5
	RL	1.217	1.240	1.229	1.247	1.227	1.2
	RE	3.322	3.313	3.313	3.303	3.313	3.3
	ratio	2.091	2.071	2.086	2.051	2.110	2.1
3 cm	LEVEL	4.072	4.082	4.078	4.097	4.085	4.1
	RL	1.277	1.279	1.286	1.280	1.276	1.3
	RE	3.367	3.347	3.368	3.359	3.340	3.4
	ratio	2.616	2.619	2.594	2.634	2.632	2.6
3.5cm	LEVEL	5.047	5.052	5.045	5.032	5.049	5.0
	RL	1.305	1.320	1.300	1.298	1.300	1.3
	RE	3.552	3.584	3.573	3.564	3.573	3.6
	ratio	3.609	3.555	3.627	3.620	3.633	3.6
4 cm	LEVEL	6.317	6.304	6.300	6.320	6.323	6.3
	RL	1.326	1.315	1.309	1.311	1.317	1.3
	RE	4.629	4.619	4.628	4.619	4.650	4.6
	ratio	4.898	4.943	4.971	4.984	4.955	4.9
4.5cm	LEVEL	7.709	7.718	7.718	7.716	7.700	7.7
	RL	1.326	1.315	1.325	1.319	1.315	1.3
	RE	6.356	6.374	6.354	6.373	6.368	6.4
	ratio	6.413	6.487	6.421	6.456	6.473	6.4

NOTE: level0 = 1.8 and Ref0 = 0.4

Similarly Table 2 collects raw results from measurement setup with the backflow control board. In the same consideration of the features as mentioned previously, all the three capacitances have a proper treatment as shown in Figure 39. However, the RE brings the problem about since it is still at high value instead.

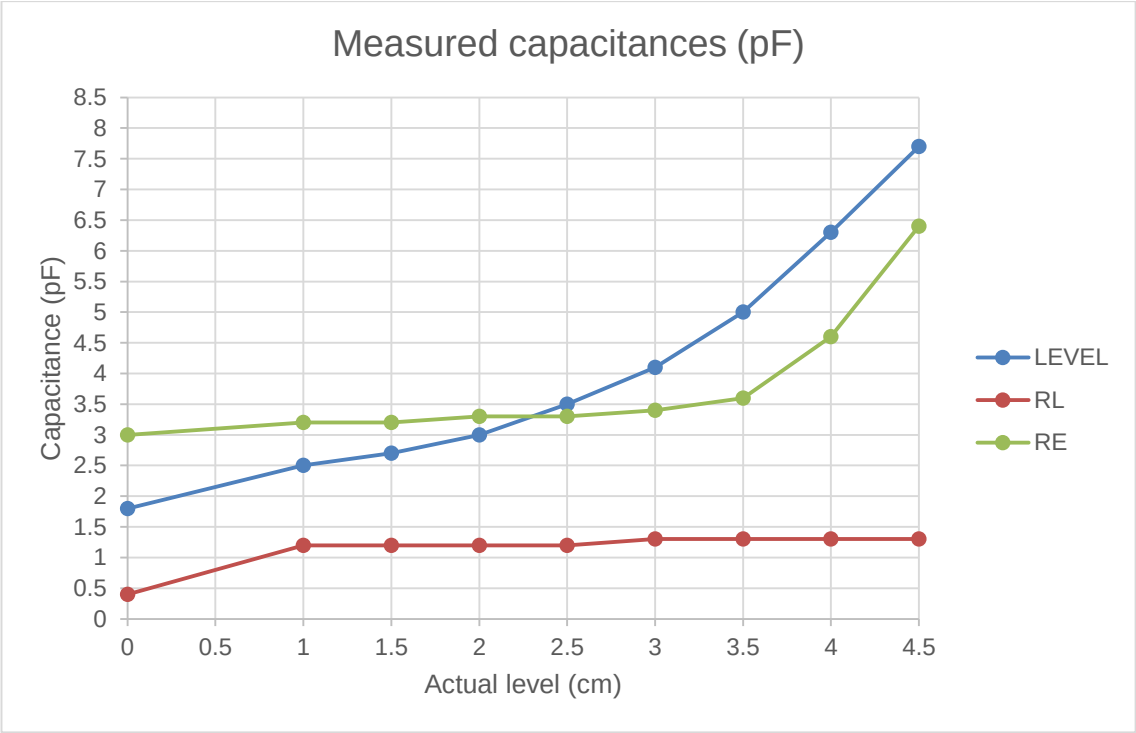

Figure 39. Capacitance measurement results with the backflow control board.

If the parasitic capacitance of the sensor connection is assumed the cause, it can be treated as an offset of 2.6pF to reduce the RE capacitance to approximate the original value of the water-free RL sensor. In this case, the differential measurement is applied in the measurement range under 3.5cm of the water level. Figure 40 indicates if corrected by a gain of 0.75, the estimated level by differential measurement is closer to the expected value but still suffers a significant error. Therefore, the RE sensor capacitance is still unknown variable to solve for the level in differential measurement.

The situation turns brighter to the application of the ratiometric measurement of the water level with no concerns of the RE sensor. Figure 41 depicts the measured level including two approximate linear sections with different tangents: one before the water level reach 3cm and the upper one. These can be calibrated to be more adjacent to the expected line, which offers a solution for an acceptable sensing accuracy as if the estimation of the linearity of the measured level is not violated every time the water full up the RE sensor space in the tank.

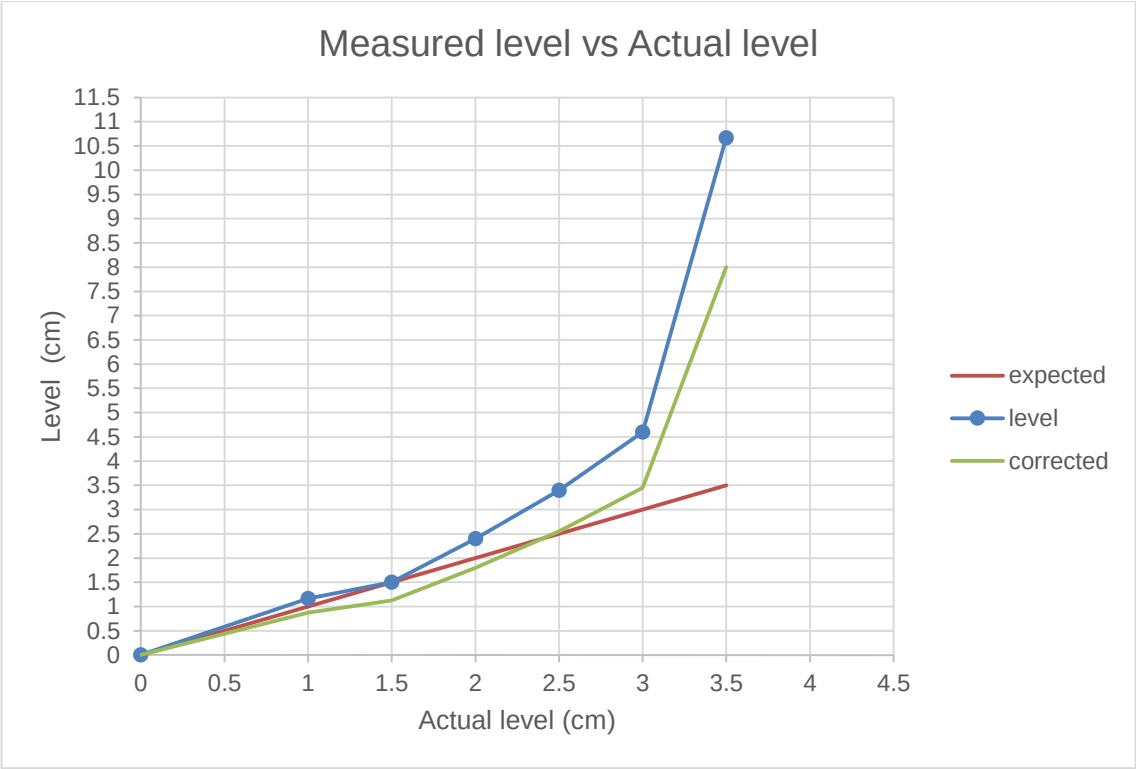

Figure 40. Estimation of the level with 2.6pF-offset RE capacitance

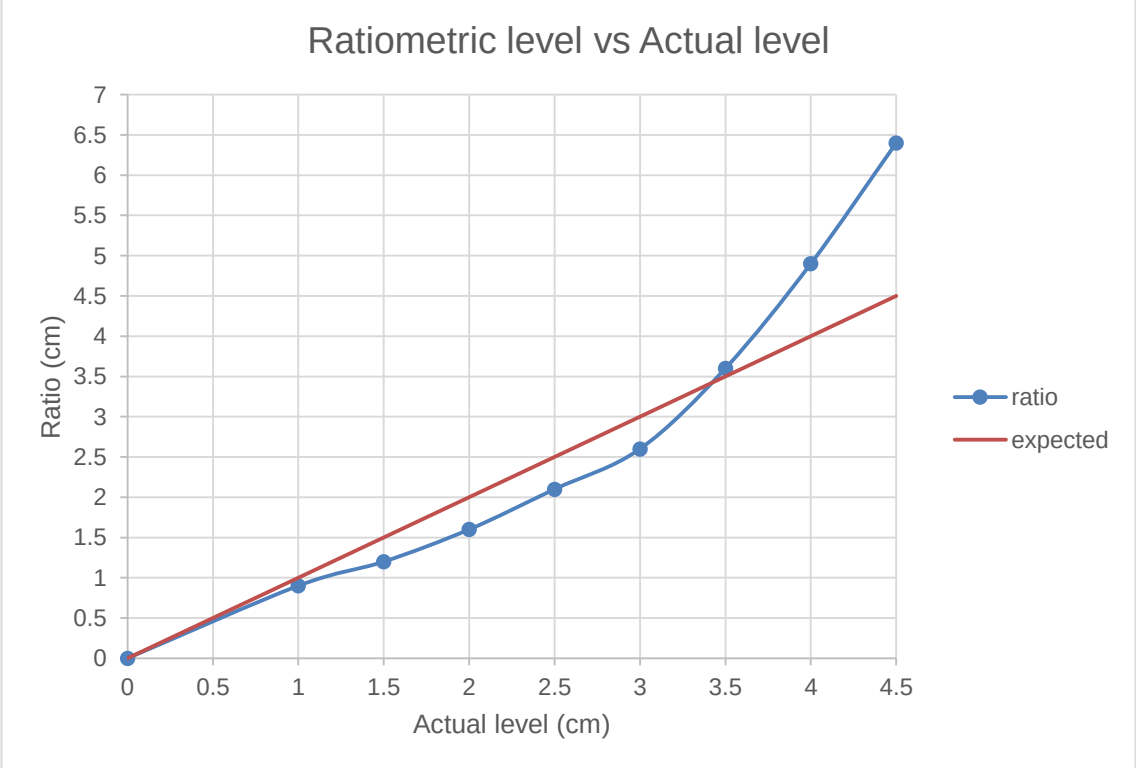

Figure 41. Ratiometric level versus actual level without the RE sensor concerned.

A calibration of the ratiometric level is shown up in Figure 42 to perfectly match the actual level. However, there is still the requirement to inspect the consistence of the linear behaviour of the measured level. For the sake of logic up till now, it is reasonable to calibrate the first section of the ratiometric level with a gain of 1.2 and the second section with +5.04 offset and a gain of 0.4.

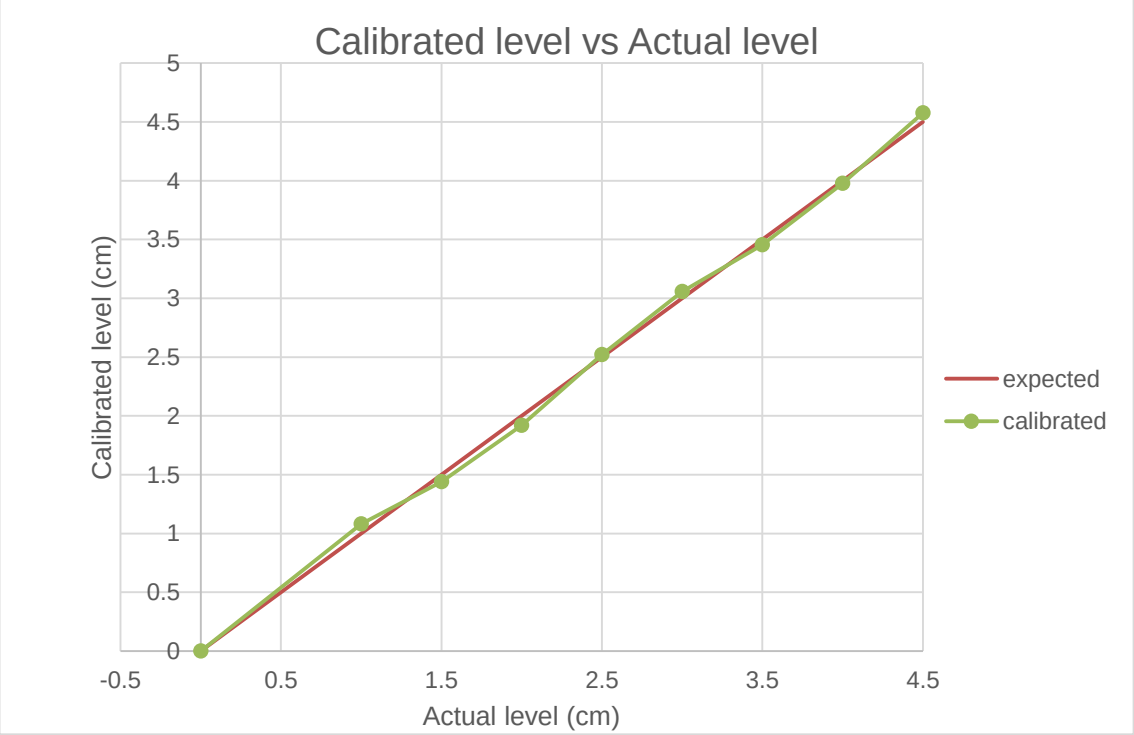

Figure 42. Measured level versus actual level without RE sensor used.

8 Conclusion

In time limit of the project, there has left a work load for further development of this subject. As discussed and suggested to produce the sensor port of a flexible-rigid PCB whereof the FDC1004 or any other replaceable CDC integrated, the prototype can be fast tested and well learnt with any MCU platform using the online ARMmbed IDE. Different capacitance measurement methods can be further studied and applied to the sensor prototype with open terminal pads designed for testing. That way offers teaching methods of technologies of electronics designs, sensors and embedded system programming. This document can be treated as a study reference for a new theoretical analysis to be extended of active shielding and capacitance to digital conversion. Deep understanding of CDC inner content can help to justify the proper behaviour of the measured liquid level by the CDC. As a dedicated and typical application guideline of the coplanar electrode capacitive sensing, it should be considered fundamental and beneficial to be referred for various applications using the same technology.

For further improvement and justification of the application of liquid level capacitive sensing OoP technology, it is supposed to re-design the system of the sensor electrodes with different trials of geometric parameters. It is believed the better linearity of the measured level depending on the longer length of the electrode relative to its gap separation and width. It actually continues proceeding this process in the practice of the development of the backflow prevention device. For a possible solution, the RE capacitor can be taken away and the water level system operates with the other capacitors: the LEVEL only referring the RL. However, this thesis work has come to an ending report here with fulfilment of numerous knowledge and experience the Electronics Engineering graduate has gained of capacitive sensors, CDC application, I^2C, mbed programming and FPC design.

References

[1] David Wang. FDC1004: Basics of Capacitive Sensing and Applications [online]. Application Report: SNOA927. Dallas, Texas, UAS: Texas Instruments; December 2014.
URL: http://www.ti.com/lit/an/snoa927/snoa927.pdf. Accessed 15 January 2016.

[2] M.F.A.Rahman, A.A.Manaf & M.R.Arshad. Capacitive effect of coplanar electrodes partially outside the microchannel region for underwater microfluidic-based sensor. Indian Journal of Geo Marine Sciences [serial online] 2013; 42(8): 987-991.
URL:
http://nopr.niscair.res.in/bitstream/123456789/25469/1/IJMS%2042%288%29%20987-991.pdf.
Accessed 30 January 2016.

[3] Alam M. Applications of electromagnetic principles in the design and development of proximity wireless sensor [Doctoral dissertation]. University of South Carolina – Columbia; September 2014.
URL:
http://scholarcommons.sc.edu/cgi/viewcontent.cgi?article=3791&context=etd.
Accessed 5 February 2016.

[4] Jian Z. Chen, Anton A. Darhuber, Sandra M. Troian & Sigurd Wagner. Capacitive sensing of droplets for microfluidic devices based on thermocapillary actuation. Lab Chip [serial online] 2004; 4: 473–480.
URL: http://www.its.caltech.edu/~stroian/papers/Chen_LabOnAChip_4_04.pdf.
Accessed 10 February 2016.

[5] Abraham Otero, Roemi Fernández, Andrey Apalkov & Manuel Armada. An Automatic Critical Care Urine Meter. Sensors [serial online] 2012; 12(10): 13109-13125.
URL: http://www.mdpi.com/1424-8220/12/10/13109/htm.
Accessed 21 February 2016.

[6] David Wang. Capacitive-Based Liquid Level Sensing Sensor Reference Design [online]. TI Designs: TIDU736A. Dallas, Texas, UAS: Texas Instruments; January 2015.
URL: http://www.ti.com/lit/ug/tidu736a/tidu736a.pdf. Accessed 29 January 2016.

[7] David Wang. Capacitive Sensing: Ins and Outs of Active Shielding [online]. Application Report: SNOA926A. Dallas, Texas, UAS: Texas Instruments; February 2015.

URL: http://www.ti.com/lit/an/snoa926a/snoa926a.pdf.
Accessed 5 March 2016.

[8] FDC1004: 4-Channel Capacitance-to-Digital Converter for Capacitive Sensing Solutions [online]. Technical Documents: SNOSCY5B. Dallas, Texas, UAS: Texas Instruments; August 2014.
URL: http://www.ti.com/lit/ds/snoscy5b/snoscy5b.pdf. Accessed 15 March 2016.

[9] David Wang. Capacitive Sensing: Out-of-Phase Liquid Level Technique [online]. Application Report: SNOA925. Dallas, Texas, UAS: Texas Instruments; January 2015.
URL: http://www.ti.com/lit/an/snoa925/snoa925.pdf. Accessed 29 January 2016.

[10] I2C and SPI [online]. Quick2Wire. Web.
URL: http://quick2wire.com/articles/i2c-and-spi. Accessed 1 May 2016.

[11] I2C Bus Specification [online]. I2C Info. Web.
URL: http://i2c.info/i2c-bus-specification. Accessed 1 May 2016.

[12] SerialPC [online]. ARMmbed. Web.
URL: https://developer.mbed.org/handbook/SerialPC. Accessed 7 May 2016.

[13] I2C [online]. ARMmbed. Web.
URL: https://developer.mbed.org/handbook/I2C. Accessed 13 May 2016.

Main code file

```
/*
main.cpp by Thao Nguyen 10.5.2016
testing the liquid level FDC1004 capacitive sensor on Nucleo-
STM32 platform
*/
#include "mbed.h"
#include "main.h"

int main()
{
  /* Configure MEAS1 = CIN1-CIN4 (0x0C), MEAS2 = CIN2-CIN4
  (0x2C), MEAS3 = CIN3-CIN4 (0x4C) with CAPDAC disable (0x00) */
  Config(CONF_MEAS1, 0x0C, 0x00);
  Config(CONF_MEAS2, 0x2C, 0x00);
  Config(CONF_MEAS3, 0x4C, 0x00);

  /* Configure FDC regster for 400sample/s, repeated mode (0x0D)
  and trigger 3 MEAS ((0xE0)*/
  //Config(FDC_CONF, 0x0D, 0xE0);

  /* read conf-registers*/
  int conf_meas1;
  int conf_meas2;
  int conf_meas3;
  int fdc_conf;

  conf_meas1 = Read_1_register(CONF_MEAS1);
  conf_meas2 = Read_1_register(CONF_MEAS2);
  conf_meas3 = Read_1_register(CONF_MEAS3);
  fdc_conf = Read_1_register(FDC_CONF);

  /* infinite loop for continuous meassurements */
  while (1)
  {
      /* set up meas1-----------------------------------------*/
```

```
/* print conf-registers reading on PC screen */
pc.printf("\nconf_meas1 = %x\t", conf_meas1);
pc.printf("conf_meas2 = %x\t", conf_meas2);
pc.printf("conf_meas3 = %x\t", conf_meas3);
pc.printf("fdc_conf = %x\r\n", fdc_conf);

/* Configure FDC regster for 400sample/s, single mode (0x0C)
and trigger MEAS1 ((0x80) */
Config(FDC_CONF, 0x0C, 0x80);

/* wait 10ms for meas1 complete */
wait(0.003);

/* check fdc-conf register if bit [3] for meas1 done is set
to 1 */
fdc_conf = Read_1_register(FDC_CONF);
pc.printf("fdc_conf = %x\r\n", fdc_conf);

/* read meas1 reasult */
int meas1_result = 0;
meas1_result = Read_Meas(MEAS1_MSB, MEAS1_LSB);

/* check fdc_conf register if bit [3] is set to 0 */
fdc_conf = Read_1_register(FDC_CONF);
pc.printf("fdc_conf = %x\r\n", fdc_conf);


/* set up the same for meas2 and meas3-------------------*/

/* Configure FDC regster for 400sample/s, single mode (0x0C)
and trigger MEAS2 ((0x40)*/
Config(FDC_CONF, 0x0C, 0x40);

wait(0.003);
```

```
fdc_conf = Read_1_register(FDC_CONF);
pc.printf("fdc_conf = %x\r\n", fdc_conf);

int meas2_result = 0;
meas2_result = Read_Meas(MEAS2_MSB, MEAS2_LSB);

fdc_conf = Read_1_register(FDC_CONF);
pc.printf("fdc_conf = %x\r\n", fdc_conf);

/* Configure FDC regster for 400sample/s, single mode (0x0C)
and trigger MEAS3 ((0x20)*/
Config(FDC_CONF, 0x0C, 0x20);

wait(0.003);

fdc_conf = Read_1_register(FDC_CONF);
pc.printf("fdc_conf = %x\r\n", fdc_conf);

int meas3_result = 0;
meas3_result = Read_Meas(MEAS3_MSB, MEAS3_LSB);

fdc_conf = Read_1_register(FDC_CONF);
pc.printf("fdc_conf = %x\r\n", fdc_conf);

/* display the results-----------------------------------*/

/* calculate sensor capacitances */
float cap1;
float cap2;
float cap3;

cap1 = ((float)(meas1_result)/0x80000);
cap2 = (float)(meas2_result)/0x80000;
cap3 = ((float)(meas3_result)/0x80000);

if(cap1 >= 16){cap1 = cap1 - 32;}
```

```
        if(cap2 >= 16){cap2 = cap2 - 32;}
        if(cap3 >= 16){cap3 = cap3 - 32;}

        /* Calculate the liquid height = 'ratio' in ratiometric mode
        (2 sensors are used), 'level' in differential mode
        (3 sensors are used) */
        float ratio;
        float level;
        float level0 = 0;
        float ref0 = 0;

        ratio = ((float)(cap1)-level0)/((float)(cap2)-ref0);
        level = ((float)(cap1)+level0) / ((float)(cap2)
                                          -(float)(cap3));

        /* Display results on PC screen */
        pc.printf("meas1_result = %x \r\n", meas1_result);
        pc.printf("meas2_result = %x \r\n", meas2_result);
        pc.printf("meas3_result = %x \r\n", meas3_result);
        pc.printf("cap1 = %f pF\r\n", cap1);
        pc.printf("cap2 = %f pF\r\n", cap2);
        pc.printf("cap3 = %f pF\r\n", cap3);
        pc.printf("ratio = %f cm\r\n", ratio);
        pc.printf("level = %f cm\r\n", level);

        /* running with no error */
        myled = !myled;
        wait(1.0);
    }
}
```

Main header file

```
/*
main.h by Thao Nguyen 10.5.2016
testing the liquid level FDC1004 capacitive sensor on Nucleo-
STM32 platform
*/

#define FDC1004_ADDRESS 0xA0

#define MEAS1_MSB 0x00
#define MEAS1_LSB 0x01

#define MEAS2_MSB 0x02
#define MEAS2_LSB 0x03

#define MEAS3_MSB 0x04
#define MEAS3_LSB 0x05

#define CONF_MEAS1 0x08
#define CONF_MEAS2 0x09
#define CONF_MEAS3 0x0A

#define FDC_CONF 0x0C

I2C i2c(I2C_SDA, I2C_SCL);

DigitalOut myled(LED1);

Serial pc(SERIAL_TX, SERIAL_RX);

static void Config(char pointer, char msb, char lsb)
{
    char Meas_conf[3] = {pointer, msb, lsb};
    int status = i2c.write(FDC1004_ADDRESS, Meas_conf, 3, 0);
```

```
    if (status != 0) { // Error
        while (1) {
            myled = !myled;
            wait(0.2);
        }
    }
};

static int Read_1_register(char pointer)
{
     char address[1];
     address[0] = pointer;
     char value[2];

     i2c.write(FDC1004_ADDRESS, address, 1, 1); // no stop
     i2c.read(FDC1004_ADDRESS, value, 2, 0);

     int result = (int)((int)value[0] << 8) | value[1];

     return result;
};

static int Read_Meas(char MEAS_MSB, char MEAS_LSB)
{
  int msb = 0;
  int lsb = 0;
  int result = 0;
  msb = Read_1_register(MEAS_MSB);
  lsb = Read_1_register(MEAS_LSB);
  result = ((msb << 8) | (lsb >> 8));
  return result;
}
```